การพัฒนาตัวรับรู้ออกซาเลตโดยใช้อุปกรณ์วิเคราะห์ฐานกระดาษ

ว่าที่ร้อยตรีหญิงมนัสวี จั่นรอด

วิทยานิพนธ์นี้เป็นส่วนหนึ่งของการศึกษาตามหลักสูตรปริญญาวิทยาศาสตรมหาบัณฑิต
สาขาวิชาเคมี ภาควิชาเคมี
คณะวิทยาศาสตร์ จุฬาลงกรณ์มหาวิทยาลัย
ปีการศึกษา 2559

DEVELOPMENT OF OXALATE SENSOR USING PAPER-BASED ANALYTICAL DEVICE

Acting Sub Lieutenant Manassawee Janrod

A Thesis Submitted in Partial Fulfillment of the Requirements

for the Degree of Master of Science Program in Chemistry

Department of Chemistry

Faculty of Science

Chulalongkorn University

Academic Year 2016

Thesis Title	DEVELOPMENT OF OXALATE SENSOR USING PAPER-BASED ANALYTICAL DEVICE
By	Acting Sub Lieutenant Manassawee Janrod
Field of Study	Chemistry
Thesis Advisor	Monpichar Srisa-Art, Ph.D.
Thesis Co-Advisor	Professor Orawon Chailapakul, Ph.D.

Accepted by the Faculty of Science, Chulalongkorn University in Partial Fulfillment of the Requirements for the Master's Degree

.....Dean of the Faculty of Science
(Associate Professor Polkit Sangvanich, Ph.D.)

THESIS COMMITTEE

.....Chairman
(Associate Professor Vudhichai Parasuk, Ph.D.)

.....Thesis Advisor
(Monpichar Srisa-Art, Ph.D.)

.....Thesis Co-Advisor
(Professor Orawon Chailapakul, Ph.D.)

.....Examiner
(Assistant Professor Suchada Chuanuwatanakul, Ph.D.)

.....External Examiner
(Yupaporn Sameenoi, Ph.D.)

มนัสวี จั่นรอด : การพัฒนาตัวรับรู้ออกซาเลตโดยใช้อุปกรณ์วิเคราะห์ฐานกระดาษ (DEVELOPMENT OF OXALATE SENSOR USING PAPER-BASED ANALYTICAL DEVICE) อ.ที่ปรึกษาวิทยานิพนธ์หลัก: ดร.มนพิชา ศรีสะอาด, อ.ที่ปรึกษาวิทยานิพนธ์ร่วม: ศ. ดร.อรวรรณ ชัยลภากุล, 87 หน้า.

งานวิจัยนี้ได้พัฒนาตัวรับรู้ออกซาเลตโดยใช้อุปกรณ์วิเคราะห์ฐานกระดาษร่วมกับการตรวจวัดทางเคมีไฟฟ้าและการตรวจวัดด้วยสี สำหรับการวิเคราะห์หาปริมาณออกซาเลตโดยใช้การตรวจวัดทางเคมีไฟฟ้าทำได้โดยการตรวจวัดผ่านไฮโดรเจนเปอร์ออกไซด์ที่เกิดขึ้นจากปฏิกิริยาระหว่างออกซาเลตกับเอนไซม์ออกซาเลตออกซิเดสที่ได้จากชุดตรวจออกซาเลตสำเร็จรูป ขั้วไฟฟ้าคาร์บอนเพสที่ใช้เป็นขั้วไฟฟ้าใช้งานจะถูกดัดแปรด้วยอนุภาคเงินระดับนาโนเมตร และท่อนาโนคาร์บอนแบบผนังหลายชั้นเพื่อเพิ่มสัญญาณทางเคมีไฟฟ้าของไฮโดรเจนเปอร์ออกไซด์ ขั้วไฟฟ้าคาร์บอนเพสจะประกอบด้วยส่วนที่เป็นน้ำมันซึ่งใช้น้ำมันแร่และพีดีเอ็มเอส กับผงแกรไฟต์ในอัตราส่วน 50 เปอร์เซ็นต์โดยน้ำหนัก ขั้วไฟฟ้าคาร์บอนเพสจะถูกดัดแปรด้วยอนุภาคเงินระดับนาโนเมตร ความเข้มข้น 10 กรัมต่อลิตร ปริมาตร 400 ไมโครลิตร และท่อนาโนคาร์บอนแบบผนังหลายชั้น ปริมาณ 1 เปอร์เซ็นต์โดยน้ำหนัก เมื่อนำขั้วไฟฟ้าที่พัฒนาขึ้นไปตรวจวัดไฮโดรเจนเปอร์ออกไซด์โดยใช้เทคนิคแอมเพอโรเมตรีที่ความต่างศักย์ -0.6 โวลต์ พบว่าให้ช่วงความเป็นเส้นตรงสองช่วงคือ 0.05-10 และ 10-1,000 มิลลิโมลาร์ จากช่วงความเป็นเส้นตรงช่วงแรก พบว่าขีดจำกัดการตรวจวัดและขีดจำกัดการวิเคราะห์เชิงปริมาณเท่ากับ 0.02 และ 0.08 มิลลิโมลาร์ ตามลำดับ การตรวจวัดออกซาเลตโดยใช้ขั้วไฟฟ้าที่พัฒนาขึ้นทำได้โดยให้ออกซาเลตทำปฏิกิริยากับเอนไซม์ออกซาเลตออกซิเดสจากรีเอเจนต์บีซึ่งประกอบด้วยเอนไซม์ออกซาเลตออกซิเดส และเอนไซม์ฮอสราดิชเปอร์ออกซิเดส อย่างไรก็ตามพบว่าไม่ปรากฏสัญญาณทางเคมีไฟฟ้าเกิดขึ้น ทั้งนี้อาจเนื่องมาจากไฮโดรเจนเปอร์ออกไซด์ที่เกิดขึ้นจากปฏิกิริยาของเอนไซม์อาจจะไปทำปฏิกิริยากับเอนไซม์ฮอสราดิชเปอร์ออกซิเดสที่ผสมอยู่ในรีเอเจนต์บี ดังนั้นจึงไม่ประสบความสำเร็จในการตรวจวัดออกซาเลตโดยใช้อุปกรณ์วิเคราะห์ฐานกระดาษร่วมกับการวิเคราะห์ทางเคมีไฟฟ้า

นอกจากนี้ยังได้พัฒนาตัวรับรู้ออกซาเลตโดยใช้อุปกรณ์วิเคราะห์ฐานกระดาษร่วมกับการตรวจวัดด้วยสีโดยใช้ปฏิกิริยาของเอนไซม์แบบเดิม ไฮโดรเจนเปอร์ออกไซด์ที่เกิดขึ้นจะไปทำปฏิกิริยากับ 3-(Dimethylamino) benzoic acid (DMAB) และ 3-Methyl-2-benzothiazolinine (MBTH) เกิดเป็นสีน้ำเงินของ Indamine ซึ่งความเข้มของสีที่เกิดขึ้นจะสัมพันธ์กับปริมาณของออกซาเลตในสารตัวอย่าง การรบกวนการตรวจวัดออกซาเลตจากกรดแอสคอบิกที่มีอยู่ในปัสสาวะจะถูกทำให้ลดลงโดยการเติมสารบดบังที่ประกอบด้วยคอปเปอร์ซัลเฟต, กรดบอริก และโซเดียมไฮดรอกไซด์ เพื่อไปทำปฏิกิริยากับกรดแอสคอบิกเป็นเวลา 30 นาที ปริมาณสารต่าง ๆ ที่เหมาะสมในการวิเคราะห์ออกซาเลตคือการใช้เอนไซม์ออกซาเลตออกซิเดส, ฮอสราดิชเปอร์ออกซิเดส, DMAB และ MBTH เท่ากับ 3×10^{-3} ยูนิตต่อลิตร, 1×10^{-4} ยูนิตต่อลิตร, 2.4 มิลลิโมลาร์ และ 0.0176 มิลลิโมลาร์ ตามลำดับ โดยให้ทำปฏิกิริยากับออกซาเลตเป็นเวลา 10 นาทีก่อนที่จะวัดความเข้มสี ช่วงความเป็นเส้นตรงของการตรวจวัดออกซาเลตอยู่ในช่วง 5-50 มิลลิกรัมต่อลิตร มีขีดจำกัดการตรวจวัดและขีดจำกัดการการวิเคราะห์เชิงปริมาณเท่ากับ 3.38 และ 11.27 มิลลิกรัมต่อลิตรตามลำดับ จากการทดลองพบว่าตัวรับรู้ออกซาเลตที่ใช้อุปกรณ์วิเคราะห์ฐานกระดาษร่วมกับการตรวจวัดด้วยสีการตรวจวัดด้วยสีสามารถตรวจวัดออกซาเลตในตัวอย่างปัสสาวะได้อย่างมีความแม่นและความเที่ยงสูง โดยมีร้อยละการกลับคืนของออกซาเลตที่เติมในปัสสาวะอยู่ในช่วง 80.7-110.0% และมีเปอร์เซ็นต์ส่วนเบี่ยงเบนมาตรฐานสัมพัทธ์ของการวิเคราะห์ปริมาณออกซาเลตภายในวันเดียวกันและต่างวันกันน้อยกว่า 5% ดังนั้นตัวรับรู้ออกซาเลตที่ใช้อุปกรณ์วิเคราะห์ฐานกระดาษที่พัฒนาขึ้นเหมาะที่จะเป็นอุปกรณ์ที่ใช้ง่าย ใช้ปริมาณสารน้อย น่าเชื่อถือและพกพาสะดวกสำหรับการตรวจวัดออกซาเลต โดยเฉพาะอย่างยิ่งการวิเคราะห์นอกสถานที่

ภาควิชา เคมี	ลายมือชื่อนิสิต .....
สาขาวิชา เคมี	ลายมือชื่อ อ.ที่ปรึกษาหลัก .....
ปีการศึกษา 2559	ลายมือชื่อ อ.ที่ปรึกษาร่วม .....

5772105123 : MAJOR CHEMISTRY

KEYWORDS: OXALATE / PAPER-BASED ANALYTICAL DEVICE / AMPEROMETRY/ COLORIMETRY

MANASSAWEE JANROD: DEVELOPMENT OF OXALATE SENSOR USING PAPER-BASED ANALYTICAL DEVICE. ADVISOR: MONPICHAR SRISA-ART, Ph.D., CO-ADVISOR: PROF. ORAWON CHAILAPAKUL, Ph.D., 87 pp.

Herein, oxalate sensors were developed using paper-based analytical devices (PADs) coupled with electrochemical and colorimetric detection. For electrochemical paper-based analytical device (ePAD), the amount of oxalate in the solution was determined through the measurement of hydrogen peroxide (H_2O_2) produced from the enzymatic reaction between oxalate and oxalate oxidase (OxOx) obtained from an oxalate test kit. A carbon paste electrode (CPE) as a working electrode (WE) was modified with silver nanoparticles (AgNPs) and multi-walled carbon nanotubes (MWCNTs) to enhance electrochemical signal of H_2O_2. A CPE was composed of 50% w/w oil phase (mineral oil and PDMS) and 50% w/w graphite powder. The CPE was modified with 400 µL of 10,000 ppm AgNPs and 1% w/w MWCNTs. The AgNPs-MWCNTs-CPE was used to measure H_2O_2 using amperometric detection with an applied potential of -0.6 V. The linear ranges of the method for determination of H_2O_2 were in the ranges of 0.05-10 and 10-1,000 mM. From the first linear range, limit of detection (LOD) and limit of quantitation (LOQ) were found to be 0.02 and 0.08 mM, respectively. For detection of oxalate using the AgNPs-MWCNTs-CPE, oxalate solution was reacted with OxOx in a reagent B consisting of OxOx and horseradish peroxidase (HRP). However, electrochemical signal was not observed, which could be because the produced H_2O_2 was reacted with HRP from the reagent B. Therefore, the electrochemical determination of oxalate using ePADs was not successful.

In addition, a PAD was developed with colorimetric detection as an oxalate sensor using the same enzymatic reaction. The produced H_2O_2 was reacted with 3-(Dimethylamino) benzoic acid (DMAB) and 3-Methyl-2-benzothiazolinine (MBTH) to produce an indamine dye which is a blue color. The color intensity corresponded to the amount of oxalate in the solution. Interfering effect of AA contained in urine was minimized by adding a masking reagent ($CuSO_4$, H_3BO_3 and NaOH) to react with AA for 30 min. The optimized amounts of OxOx, HRP, DMAB and MBTH were 3×10^{-3} u L^{-1}, 1×10^{-4} u L^{-1}, 2.4 mM and 0.0176 mM, respectively, which were used to react with oxalate for 10 min before measuring color intensity. The linearity of the method was in the range of 5-50 ppm. LOD and LOQ were found to be 3.38 and 11.27 ppm, respectively. The developed oxalate sensor based on PADs with colorimetric detection was successful to determine oxalate in urine with high accuracy and precision, in which %recovery of spiked oxalate in urine was found in the range of 80.7-110.0% and %RSD values of the amounts of oxalate from intra and inter-day measurements were lower than 5%. Therefore, the developed oxalate sensor based on PADs will hold a great promise to be a simple, low-sample and reagent volume, reliable and portable tool for determination of oxalate, especially for on-site measurements.

Department: Chemistry
Field of Study: Chemistry
Academic Year: 2016

Student's Signature .....
Advis□□□□ .....
Signature
Co-Advisor's Signature .....

ACKNOWLEDGEMENTS

Firstly, I would like to express my deepest appreciation to my advisor, Dr. Monpichar Srisa-Art, for her encouragement, kindness, carefulness, assistance and suggestion all the time for research and writing of this thesis and way of my life in master degree. Moreover, special thanks to my co-advisor, Professor Dr. Orawon Chailapakul, for giving me an opportunity to present my research work in various conferences and also the help and advice.

Besides my advisors and co-advisor, I would also like to thank Associate Professor Dr. Vudhichai Parasuk, Assistant Professor Dr. Suchada Chuanuwatanakul and Dr. Yupaporn Sameenoi for being my committee and giving me guidance.

In addition, I would like to thank Dr. Poomrat Rattanarat and Assistant Professor Dr. Kanet Wongravee for their encouragement, help and great suggestion during research time.

I gratefully acknowledge the financial support from the Science Achievement Scholarship of Thailand (SAST), the 90th anniversary of Chulalongkorn University Fund, Thailand Research fund through Research Team Promotion Grant (RTA5780005) and Optical Spectroscopy and Electrochemistry Research Unit (EOSRU).

For my laboratory members and EOSRU members, thank you for providing necessary supports and helpful advice during my M.Sc. study. I appreciated friendship and meaningful suggestion of you all.

Finally, I would like to thank the important persons in my life. Without my family, I would not have been accomplished anything in my life. I always treasure your blessing, encouragement and unconditional love.

CONTENTS

Page

Page

Page

Page

Page

LIST OF TABLES

Page

LIST OF FIGURES

Page

LISTS OF ABBREVIATIONS

%RSD	Percentage of relative standard deviation
A	Electrode area
AA	L-Ascorbic acid
AgNPs	Silver nanoparticles
ALB	Albumin
BSA	Bovine serum albumin
C	Concentration
CA	Citric acid
CE	Capillary electropholysis
CE	Counter electrode
CL	Chemiluminescence
CPE	Carbon paste electrode
Cr	Creatinine
CV	Cyclic voltammetry
D	Diffusion coefficient
DMAB	3-(Dimethylamino) benzoic acid
DSLR	Digital single lens reflex
ECL	Electrochemiluminescence
EDX	Energy-dispersive X-ray spectroscopy
E_p	Peak potential
E_{pa}	Anodic peak potential

ePAD	Electrochemical paper-based analytical device
E_{pc}	Cathodic peak potential
HPLC	High-performance liquid chromatography
HRP	Horseradish peroxidase
GC	Gas chromatography
IC	Ion chromatography
i_p	Peak current
i_{pa}	Anodic peak current
i_{pc}	Cathodic peak currents
LC	Liquid chromatography
ln	Natural logarithm
JPEG	Joint photographic experts group
LOD	Limit of detection
LOQ	Limit of quantitation
MBTH	3-Methyl-2-benzothiazolinine
MWCNTs	Multi-walled carbon nanotubes
ν	Scan rate
n	Number of electron
OxOx	Oxalate oxidase
PAD	Paper-based analytical device
PBS	Phosphate buffer saline
PDMS	Polydimethylsiloxane
RE	Reference electrode
S/B	Signal to background ratio

SD	Standard deviation
SEM	Scanning electron microscope
SIA	Sequential injection analysis
SPE	Screen printed electrode
sRGB	Standard red green blue
TMBZ	Tetramethylbenzidine
WE	Working electrode
UA	Uric acid

CHAPTER I
INTRODUCTION

1.1 Introduction

Kidney stone is one of the health problems worldwide. In Thailand, the disease is mostly found in the northeast of Thailand and caused by the formation of mineral crystalline in the urinary system. The amount of mineral crystalline at high levels can form stones in the urinary tract system, such as kidney, ureter and urinary bladder, which leads to backache, blood in urine, uroschesis and renal deterioration. Therefore, determination of oxalate in the urine excretion is necessary for medical diagnosis and treatment. Although there are many stone types, such as calcium oxalate, calcium phosphate, uric acid, struvite and cystine stones, calcium oxalate is the major stone type found in patients. For healthy people, the amount of oxalate in urine of is not over 40 ppm [1, 2].

Various analytical methods have been developed to determine the amount of oxalate in urine, such as capillary electrophoresis (CE) [3], high-performance liquid chromatography (HPLC) [4], ion chromatography (IC) [5], liquid chromatography (LC) [6], spectrophotometry [7], gas chromatography (GC) [8] and fluorescence [9]. However, these methods have many disadvantages, such as expensive and complicated instrumentation, time consuming, less sensitive, large reagent and sample volume consumption, requirement of highly trained staff and difficulty for remote area [10].

Oxalate biosensors based on the enzymatic reaction between oxalate and oxalate oxidase (OxOx) [10, 11] is an interesting method to determine oxalate due to its selectivity, reliability, sensitivity and rapidity. The analysis is usually determined from products generated by the enzymatic reaction in the presence of oxygen as follows:

$$H_2C_2O_4 + O_2 \xrightarrow{OxOx} 2CO_2 + H_2O_2 \quad (1.1)$$

According to Equation 1.1, the amount of oxalate can be indirectly determined by measuring pH, which corresponds to the amount of CO_2 generated from the enzymatic reaction. Furthermore, oxalate concentration can be indirectly measured from the amount of generated H_2O_2 which can be measured using various methods, such as spectrophotometry [12] and electrochemistry [13]. Electrochemical detection is mostly used because it can directly determine the produced H_2O_2.

Mishra et al. [10] reported the development of a biosensor by immobilizing OxOx onto a carbon paste electrode (CPE) as a working electrode (WE). Oxalate was reacted with the immobilized OxOx to generate H_2O_2, as shown in Equation 1.1. When applying a potential of 0.4 V for amperometric measurements, the generated H_2O_2 was oxidized to be hydrogen ions, oxygen and electrons, as shown in Equation 1.2. The current signal obtained from the flow of electrons corresponded to the amount of oxalate in the solution. The limit of detection (LOD) was found to be 3.5 ppm, which was lower than that of glassy carbon electrode modified with OxOx [14].

$$H_2O_2 \xrightarrow{0.4\ V} 2H^+ + O_2 + 2e^- \quad (1.2)$$

Rodriguez et al. [11] reported the development of an oxalate sensor for determination of oxalate in urine using the combination of biosensor and sequential injection analysis (SIA) based on the enzymatic reaction. OxOx was immobilizied onto magnetic solid on the electrode surface, which was modified with an Fe(III)-tris(2-thiopyridone)borate complex as a mediator. The LOD was found to be 1.0 ppm.

Furthermore, solid electrodes were also used as a WE for determination of oxalate in urine, such as Au [15, 16] and Pt [17]. Although an Au electrode is mostly used, it is an expensive metal. Gold nanoparticles (AuNPs) are interesting materials to be used to modify a WE for determination of oxalate in urine [18, 19]. This was

because a WE modified with nanoparticles could enhance electrochemical signal due to its higher electrode surface area.

Afraz et al. [20] reported the development of H_2O_2 sensor using silver nanoparticles (Ag-NPs) and multi-walled carbon nanotube (CNT) modified on a glassy carbon (GC) electrode. Although the electrochemical signal of H_2O_2 was enhanced when using Ag-NPs/GC or CNT/GC as a WE, Ag-NP/CNT/GC provided the highest electrochemical signal of H_2O_2, as shown in Figure 1.1. This was because of the synergistic effect of the mixed composition of MWCNTs and AgNPs [21].

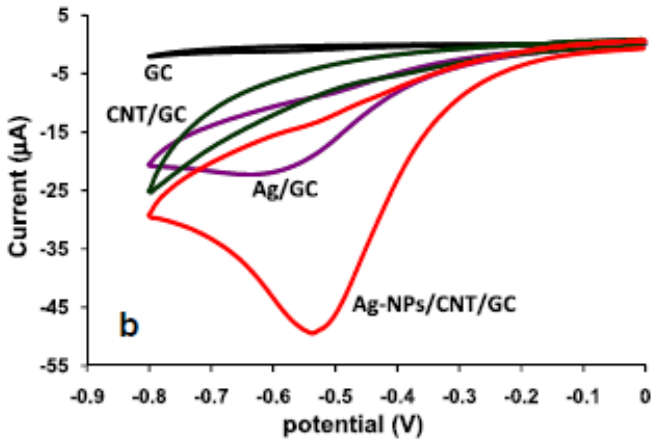

Figure 1.1 Cyclic voltammograms of 1.5 mM H_2O_2 in PBS at a bare GC, CNT/GC, Ag-NPs/GC and Ag-NPs/CNT/GC using a scan rate of 50 mV s^{-1}. Reproduced from reference [20].

Nowadays, paper-based analytical devices (PADs) have been developed for analysis in various fields, such as diagnostic test [22], food safety control [23], drug analysis [24], cell analysis [25] and environmental monitoring [26]. This is because of many advantages of PADs, such as low cost, easy process, rapid analysis, reliability, low reagent and sample volume consumption, disposability, and portability [27]. Furthermore, solution can flow without external force by capillary force through the paper as a hydrophilic material. Therefore, PADs are suitable devices to be used in developing countries and remote areas. Various detection methods have been

developed for PADs, such as colorimetry [28], electrochemistry [29], chemiluminescence (CL) [30], fluorescence [31] and electrochemiluminescence (ECL) [32]. Electrochemistry and colorimetry were widely used as detection methods for PADs because they are suitable to combine with PADs for on-site measurements [27].

Canales et al. [33] reported the development of a point-of-care device or oxometer from a commercial glucometer for determination of oxalate in synthetic urine. Glucose test strips, which were made from paper, were impregnated with OxOx and then dipped into synthetic urine in a cuvette containing various concentrations of oxalate. Oxalate was reacted with OxOx in the presence of O_2 to generate CO_2 and H_2O_2, as shown in Equation 1.1. After that, the generated H_2O_2 was reacted with tetramethylbenzidine (TMBZ) dye in the presence of horseradish peroxidase (HRP) to produce a dimer of oxidized TMBZ, which provided blue-green color, as shown in Equation 1.3. The obtained color intensity corresponded to the amount of oxalate in the sample solution.

$$H_2O_2 + \text{Tetramethylbenzidine (TMBZ)} \xrightarrow{\text{HRP}} \text{Oxidized TMBZ dimer (blue-green)} \quad (1.3)$$

Although paper could use as a substrate for determination of oxalate in urine in previous work, there was no report on development of PADs for determination of oxalate in urine. In this work, PADs coupled with electrochemical and colorimetric detection were developed for determination of oxalate in urine. An oxalate kit was used as a source of the enzyme OxOx for determination of oxalate.

PADs with electrochemical detection was developed using screen printed CPEs for determination of oxalate through H_2O_2 produced from the enzymatic reaction. CPEs were used because of the advantages including small size, easy fabrication, low cost, wide potential window and easy modification with other materials [34]. In addition, the smaller size of CPE provided less analysis time because the mass transfer rates was higher when measuring low current and lower resistance [35]. CPEs were modified with AgNPs and MWCNTs, which were reported

previously that they could enhance electrochemical signal of H_2O_2 because they increase the electrode surface area [20].

Furthermore, PADs coupled with colorimetric detection was also developed based on the same enzymatic reaction. The mixed solutions of MBTH and DMAB were used to react with H_2O_2 generated from the enzymatic reaction in the presence of HRP to form an indamine dye (blue color). The obtained color intensity corresponded to the amount of oxalate in the solution. Therefore, quantitative analysis of oxalate was performed using the measurement of color intensity from the enzymatic reaction.

1.2 Objectives of This Work

1. To develop an oxalate sensor using paper-based analytical devices coupled with electrochemical or colorimetric detection.

2. To apply the developed oxalate sensor for determination of oxalate in urine.

1.3 Scope of This Work

PADs for determination of oxalate in urine based on the enzymatic reaction were developed using colorimetric and electrochemical detection.

For determination of oxalate in urine using electrochemical detection, electrochemical paper-based analytical devices (ePADs) were fabricated using a screen printed CPE. Then, the CPE was modified with AgNPs and MWCNTs as a working electrode (WE) for determination of H_2O_2 produced from the enzymatic reaction between oxalate and OxOx. The ratio of oil phase and graphite powder mixture and the amounts of AgNPs and MWCNTs were optimized for electrode fabrication. An applied potential for amperometric measurements was also studied. In addition, the analytical performance of this method, including linearity, limit of

detection and limit of quantitation, was studied using amperometric measurements. After that, the proposed ePADs were applied to detect oxalate in urine.

Furthermore, an oxalate sensor based on PADs coupled with colorimetric detection was also developed using the same enzymatic reaction. The experimental parameters were studied to obtain the best condition for colorimetric determination of oxalate. After that, the analytical performance, including linearity, limit of detection, limit of quantitation, accuracy and precision, was studied. The selectivity of this method was also investigated. Finally, the developed oxalate sensor based on PADs with colorimetric detection was used to determine the amount of oxalate in urine samples.

CHAPTER II
THEORY

2.1 Paper-Based Analytical Device

Paper-based analytical devices (PADs) were first introduced in 2007 by Whitesides and co-workers [36]. The use of paper as a substrate of analytical devices is interesting due to its properties, such as flexibility, lightweight, fibrous and porous structure, high surface-to-volume ratio, compatible with biological samples and biodegradable materials [37]. Therefore, PADs provide many advantages, such as low cost, easy use, portability, rapid analysis and repeatability. In addition, the paper surface can be modified with several function groups for a variety of applications and fluid can flow freely without mechanical pumping due to the wicking property of the porous texture of paper [27, 38]. These advantages result in the applications of PADs in many fields, such as clinical diagnostics [22], environmental monitoring [26] and food safety control [23].

2.2 Fabrication Method

The fabrication of PADs is based on the creation of hydrophobic barrier into paper as a hydrophilic substrate to obtain micron-scale (100-1,000 μm) capillary channels for reagents flowing and detection [27, 37, 39]. Currently, various fabrication methods have been developed to fabricate PADs, including wax drawing [40], polymer ink drawing/stamping [41], wax stamping [42], wax dipping [43], photolithography [44], wax screen-printing [45], wax printing [46], inkjet etching [47], inkjet printing [48], flexographic printing [49], craft cutter [50] and laser cutter [51]. The schematics of each fabrication method are shown in Figure 2.1.

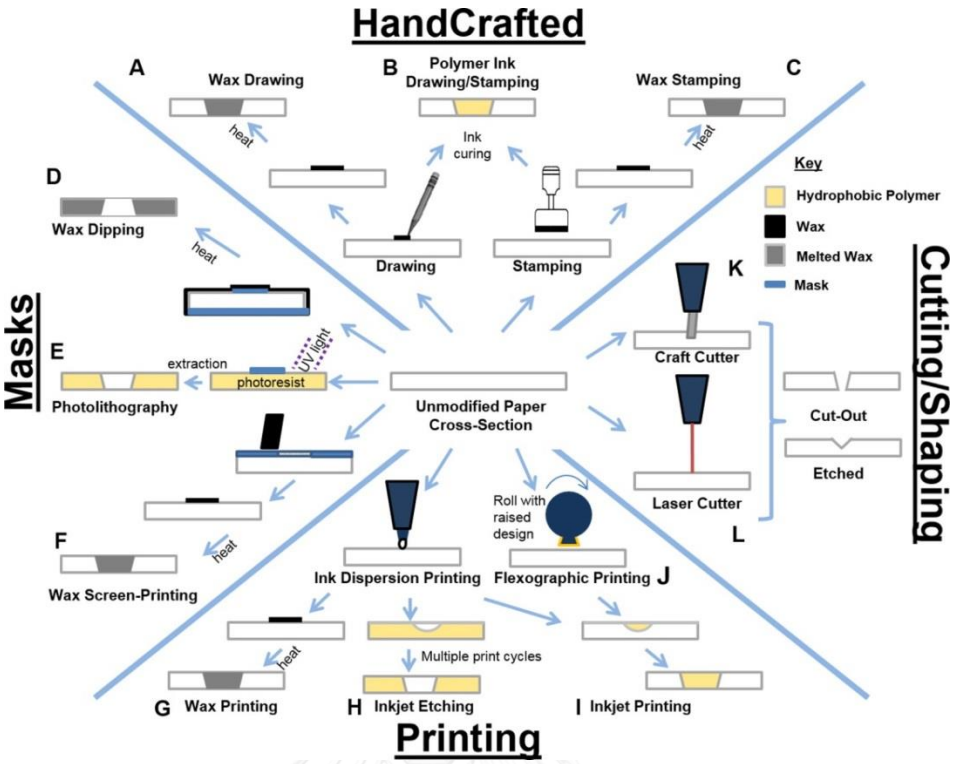

Figure 2.1 Schematics of device fabrication using various fabrication methods, which are (A) wax drawing, (B) polymer ink drawing/stamping, (C) wax stamping, (D) wax dipping, (E) photolithography, (F) wax screen-printing, (G) wax printing, (H) inkjet etching, (I) inkjet printing, (J) flexographic printing, (K) craft cutter and (L) laser cutter. Reproduced from reference [52].

In this work, wax printing was selected as a fabrication method for PADs. Wax printing is a simple fabrication method based on printing wax on paper and melting the printed wax through the porous of paper. Initially, the designed pattern was printed onto filter paper using a wax printer and then the printed paper was then placed on a hot plate to melt wax. The wax was diffused through the paper and formed as a hydrophobic barrier, whereas the other area is hydrophilic. The whole fabrication procedure is shown in Figure 2.2. The wax printing method has the following advantages; a simple and rapid process (only printing and melting wax which is approximately 5-10 min in total), inexpensive and environmentally friendly method because the process does not use organic solvents [38].

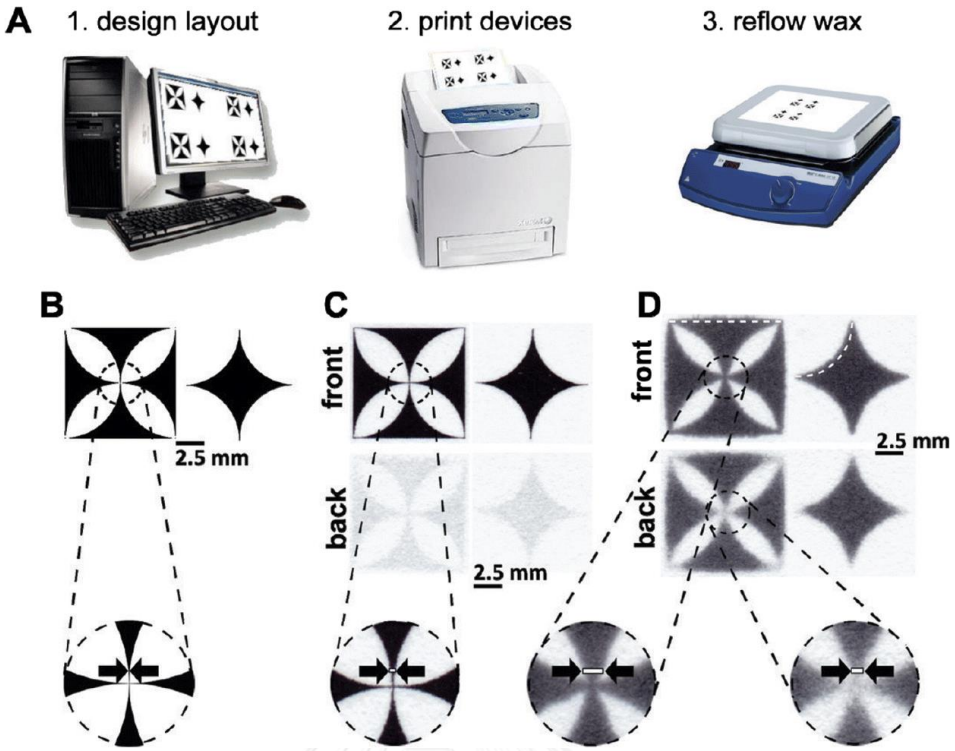

Figure 2.2 Schematic represents a wax printing process. Reproduced from reference [53].

2.3 Detector for PADs

Detection methods widely used for PADs are colorimetric [28] and electrochemical (EC) [29] detection methods.

2.3.1 Colorimetric Detection

Colorimetric detection is the simplest detection method to be coupled with PADs due to its flexibility and easy process. The color change obtained from the enzymatic or chemical reactions is monitored. In the past, the use of PADs coupled with colorimetric detection has been widely used for semi-quantitative analysis. For quantitative analysis, the color intensity change can be measured using a digital camera, camera phone or scanner and then interpreted using imaging software, such as Adobe Photoshop and ImageJ. An example of colorimetric

detection process is shown in Figure 2.3. Therefore, PADs coupled with colorimetric detection are suitable to be used in remote areas or developing countries [27, 54].

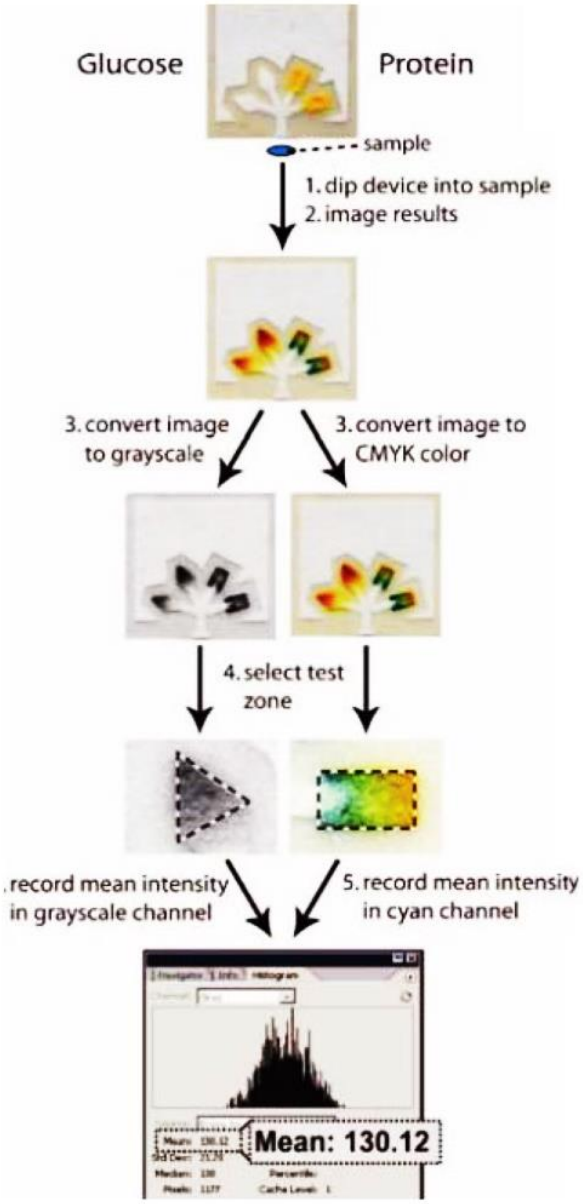

Figure 2.3 An example of colorimetric detection procedure for the determination of glucose and protein using Adobe Photoshop for color intensity interpretation. Reproduced from reference [54].

However, colorimetric detection is not sufficiently accurate because various parameters affect the color intensity, such as external light, dry or wet solutions, illumination area and background selection [54]. Therefore, electrochemical detection is an alternative to be coupled with PADs for quantitative analysis because this method provides higher accuracy and selectivity when compared with colorimetric detection.

2.3.2 Electrochemical Detection

Although it is more expensive than colorimetric detection, many advantages of electrochemical detection are still interesting, such as less analysis time and high sensitivity and selectivity [55]. Electrochemical detection can be chosen from various modes, such as potentiometry, vomtammetry, coulometry and amperometry [56]. In this work, cyclic voltammetry (CV) and amperometry were used for optimization of all parameters for electrode fabrication and sample measurements, respectively.

2.3.2.1 Cyclic Voltammetry

Cyclic voltammetry (CV) is an important and widely used electroanalytical technique [57, 58]. Generally, CV is widely used for qualitative analysis, such as the study of redox redaction of electroactive species. The principle of CV is varying applied potential as a triangular wave format in both forward and reverse directions, as shown in Figure 2.4 (a), and measuring the current. The scanned potential can be one or several cycles of triangular waveform. The initial scan direction can be negative or positive depending on sample composition. Important parameters for CV consist of cathodic peak potential (Epc), anodic peak potential (E_{pa}), cathodic peak current (i_{pc}) and anodic peak current (i_{pa}), as shown in Figure 2.4 (b). Reduction reactions occur when using negatively applied potentials and provide E_{pc} and i_{pc}. Similar to reduction reaction, oxidation reactions occur when using positively applied potentials and provide E_{pa} and i_{pa}. For a reversible reaction, the

absolute values of i_{pc} and i_{pa} should be equal but opposite in sign. In addition, the difference of peak potential (Δ_{Ep}) between E_{pa} and E_{pc} of a reversible reaction at 25 $^{\circ}$C is expected to be 0.059/n, as shown in Equation 2.1, where n is the number of electron involved in the half reaction:

$$\Delta E_p = | E_{pa} - E_{pc} | = 0.059/n \quad (2.1)$$

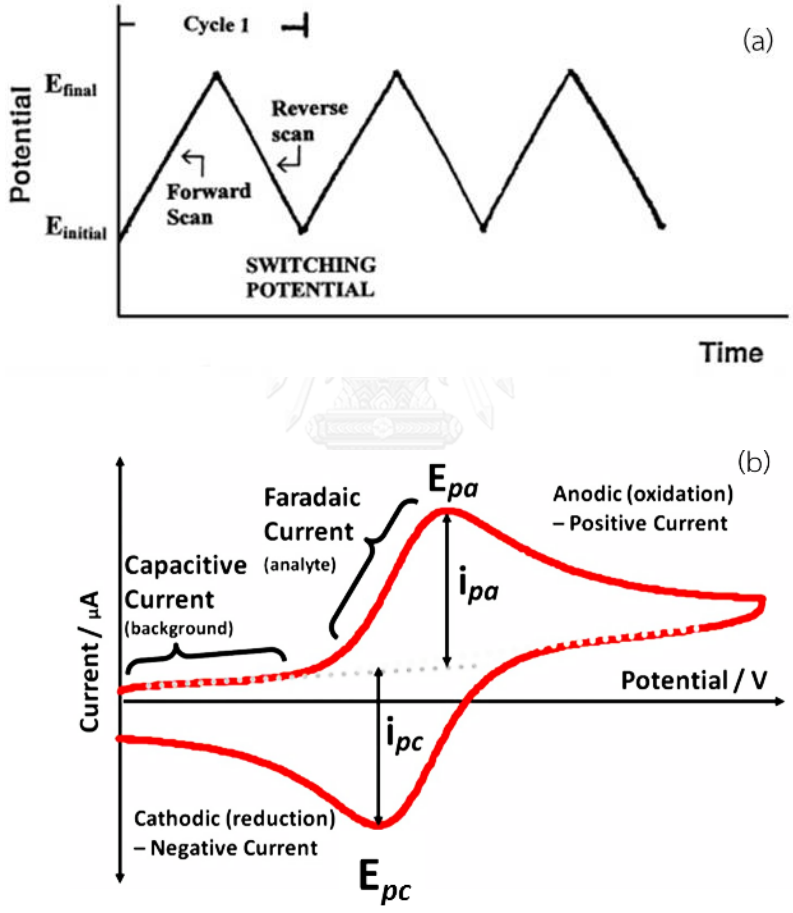

Figure 2.4 (a) Cyclic voltammogram waveforms and (b) a cyclic voltammogram of a reversible reaction. Reproduce from references [59] and [60], respectively.

At 25 ^{o}C, the peak current corresponds to the concentration of analyte according to the Randles-Sevcik equation as follow:

$$i_p = 2.686 \times 10^5 n^{3/2} ACD^{1/2} \nu^{1/2} \quad (2.2)$$

Where i_p = peak current (A)

n = number of electron

A = electrode area (cm^2)

C = concentration (mol cm^{-3})

D = diffusion coefficient (cm^2 s^{-1})

ν = scan rate (V s^{-1})

2.3.2.2 Amperometry

Amperometric detection has been widely used as an electrochemical detection method [10, 15-17]. The principle of amperometry is applying a constant potential and measuring the output current as a function of time [61, 62]. The current output is proportional to the amount of analyte in the solution. The optimum applied potential is obtained from a hydrodynamic voltammogram, which is constructed by plotting signal/background (S/B) ratio as a function of applied potential. The applied potential provides the highest S/B ratio is selected as an optimum applied potential for amperometric measurements. This technique provides good selectivity due to the selection of an applied potential, which minimizes the interfering effect from background and interference responses.

CHAPTER III

EXPERIMENTAL

3.1 Instrument and Equipment

Table 3.1 List of Instruments and equipment.

Instruments and equipment	Companies
1. Whatman filter paper (Grade No. 1)	GE Healthcare (UK)
2. Xerox Color Qube 8570 wax printer	Xerox (Japan)
3. Hotplate	IKA (Thailand)
4. Laser cutter	OHM LASER & CUTTING TOOL (China)
5. Adhesive tape	Scotch Industrial Co., Ltd., (Thailand)
6. Double-sided adhesive tape	Scotch Industrial Co., Ltd., (Thailand)
7. Membrane double-sided adhesive tape (3.2 mm thick)	Scotch Industrial Co., Ltd., (Thailand)
8. Syringe needle	NIPRO (Thailand)
9. Puncher (8 mm diameter)	Robbins Instruments, Inc. (India)
10. Potentiostat (ED410, 410-088)	Eppendorf (Thailand)
11. Micropipette (10, 100 and 1000 µL)	Eppendorf (Thailand)
12. Safe-lock tubes (200 µL and 1.5 mL)	Eppendorf (Thailand)
13. Analytical balance (5 digit)	METTLER (Canada)
14. pH meter	Mettler Toledo (Canada)
15. Rubber	Chaiyaboon Brother Co.,Ltd. (Thailand)

Instruments and equipment	Companies
16. Volumetric flask	PVG INTERNATIONAL (India)
17. Digital camera (Nikon DSLR D5300)	Nikon (Thailand)
18. Studio lightbox	UDIOBOX (Thailand)
19. Sonicator	Ultrasonic steri-cleaner
20. Nylon Syringe filter (0.2 μm)	FILTREX

3.2 Chemicals

Table 3.2 List of chemicals.

Chemicals	Companies
1. Sodium oxalate ($Na_2C_2O_4$)	Baker Analyzed (USA)
2. Oxalate kit	Trinity Biotech (Ireland)
Reagent A	
3.2 mM 3-(Dimethylamino) benzoic acid (DMAB)	
0.22 mM 3-Methyl-2-benzothiazolinine (MBTH)	
Regent B	
3000 u L^{-1} Oxalate oxidase (OxOx, Barley)	
100 u L^{-1} Horseradish Peroxidase (HRP)	
3. Phosphate buffer saline (PBS)	Sigma-Aldrich (Singapore)
4. Urea	Sigma-Aldrich (Singapore)
5. L-Ascorbic acid (AA)	BDH Analar (England)
6. Uric acid (UA)	Wako (Japan)
7. Citric acid (CA)	Riedel-de Haën (China)

Chemicals	Companies
8. Creatinine (Cr)	Sigma-Aldrich (Singapore)
9. Bovine serum albumin (BSA)	Sigma-Aldrich (Singapore)
10. Copper(II) sulphate ($CuSO_4$)	BDH Analar (UK)
11. Hydrochloric acid (HCl)	Merck (Germany)
12. Boric acid (H_3BO_3)	Merck (Germany)
13. Sodium hydroxide (NaOH)	Merck (Germany)
14. Mineral oil	Perkin Elmer (Thailand)
15. Poly dimethyl siloxane (PDMS)	Dow Corning Coporation (USA)
16. Graphite powder (≤100 μm)	Sigma-Aldrich (Singapore)
17. Silver nanoparticles (AgNPs, 10,000 ppm)	Prime Nanotechnology Co., Ltd. (Thailand)
18. Multi-walled carbon nanotubes (MWCNTs)	Chiangmai University (Thailand)
19. Silver/silver chloride (Ag/AgCl) ink	Gwent Group (UK)
20. Nitric acid (HNO_3)	Merck (Germany)
21. Sodium chloride (NaCl)	Merck (Germany)
22. Potassium chloride (KCl)	Merck (Germany)
23. Sodium hydrogen phosphate (Na_2HPO_4)	Merck (Germany)
24. Potassium dihydrogen phosphate (KH_2PO_4)	Carlo Erba Reagenti-SpA (France)
25. Deionized water (Milli-Q Gradient)	Millipore (Thailand)
26. Hydrogen peroxide (H_2O_2)	Merck (Germany)

To activate the surface of MWCNTs, an acid washing method was used to prepare MWCNTs for electrode modification. The MWCNTs were immersed in 2 M HNO_3 and stirred for 20 h. After that, the solution was filtered through No.1 Whatman filter paper and washed using Milli-Q water until the filtrate was neutralized. The MWCNTs were dried in an oven at 80 $^{\circ}C$ for 24 hr.

Part I Electrochemical Detection

3.3 Fabrication of Electrochemical Paper-Based Analytical Devices (ePADs)

The patterns of ePADs and masks were designed by CorelDraw X7 program with a dimension of 1.5 x 4.32 cm.

3.3.1 Mask Fabrication

A mask was fabricated for electrode screening onto ePADs. The designed mask consisted of a working electrode (WE) positioned opposite to a reference electrode (RE) and a counter electrode (CE), as shown in Figure 3.1 (a). The designed masks were laser printed onto a transparency film. After that, the black area of the masks on the transparency film was cut off using a laser cutter.

3.3.2 ePAD Fabrication

The pattern of an ePAD consisting of 1 cm diameter hydrophilic reservoirs (white area) surrounded by a hydrophobic barrier (black area), as shown in Figure 3.1 (b). The designed ePADs were wax printed onto No.1 Whatman filter paper. The printed ePADs were heated using a hotplate at 150 $^{\circ}$C for 15 s to melt wax through the filter paper to be a hydrophilic barrier. The backside of the heated ePADs was attached with an adhesive tape to prevent solution leakage. After that, Ag/AgCl ink and carbon paste were screened onto the ePADs in the same reservoir to serves as a RE and a CE, respectively. Carbon paste was also screened onto the other reservoir of the ePAD to serve as a WE. The ePADs with screen printed electrodes (SPEs) were heated in the oven at 55.5 $^{\circ}$C for 2 hr to dry these electrodes. The paper area between RE and CE was punched using a needle to create a 1 mm diameter hole for adding solution. The ePAD was folded in half and double-sided adhesive tape was used to stick both halves of the ePADs. Before folding, the tape was

punched to have a 0.8 mm diameter hole to create a reservoir. The overall fabrications of ePADs for determination of oxalate are shown in Figure 3.2.

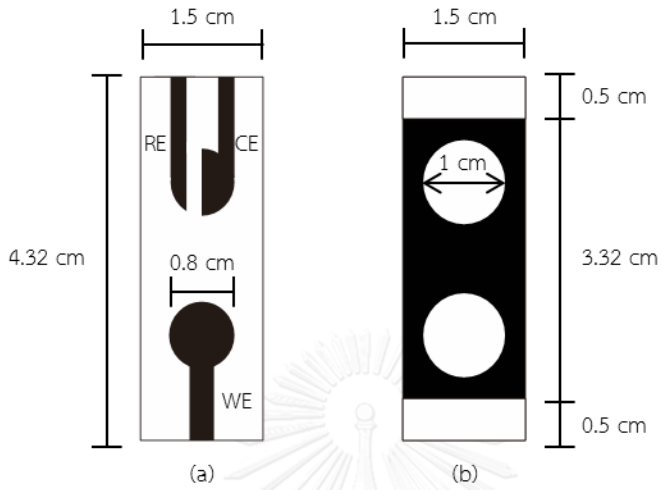

Figure 3.1 Composition of an ePAD designed using CorelDraw X7. (a) A mask for electrode fabrication and (b) reservoirs of an ePAD.

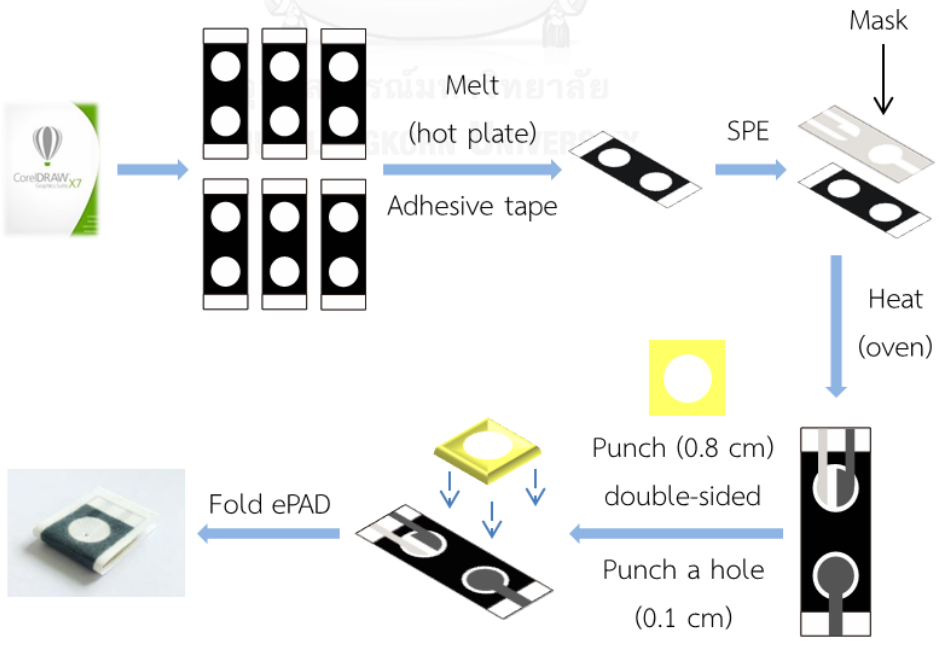

Figure 3.2 A schematic representation of the fabrication of ePADs.

3.4 Experimental Setup of Oxalate Sensor

As shown in Figure 3.3, the fabricated electrodes on an ePAD were connected to a potentiostat using alligator clips. All solutions were pipetted through a hole of an ePAD into the reservoir. After that, electrochemical measurements were performed using the optimized conditions to measure current signal.

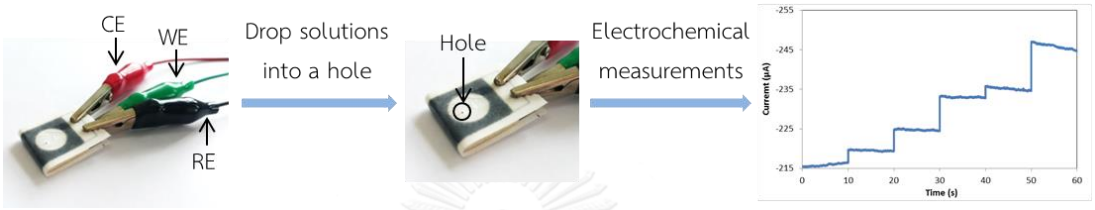

Figure 3.3 Experimental procedures of an oxalate sensor based on ePADs with electrochemical detection.

3.5 Solution Preparation

3.5.1 0.1 M KCl

A KCl solution at a concentration of 0.1 M was prepared by dissolving 6.6 mg KCl in Milli-Q water. The total volume was adjusted to 100 mL in a volumetric flask.

3.5.2 Potassium Hexacyanoferrate(III) ($K_3Fe(CN)_6$)

A $K_3Fe(CN)_6$ stock standard solution at a concentration of 100 mM was prepared by dissolving 32.92 mg $K_3Fe(CN)_6$ in 0.1 M KCl. The total volume was adjusted to 1 mL in a safe-lock tube.

For preparation of 10 mM $K_3Fe(CN)_6$, 100 µL of the $K_3Fe(CN)_6$ stock standard solution was pipetted into a safe-lock tube. The total volume was adjusted to 1 mL using 0.1 M KCl.

3.5.3 Phosphate Buffer Saline (PBS)

In this work, PBS was prepared at a concentration of 0.1 M. To prepare PBS, 4.00 g NaCl, 0.10 g KCl, 0.072 g Na_2HPO_4 and 0.12 g KH_2PO_4 were dissolved in Milli-Q water. The pH was adjusted to 7.4 using 0.1 M HCl or NaOH.

3.5.4 Hydrogen Peroxide (H_2O_2) Standard Solution

H_2O_2 stock standard solutions at concentrations of 20 and 0.1 mM were separately prepared by pipetting 2.04 and 0.1 µL of 30% H_2O_2, respectively, into safe-lock tubes. The total volume was adjusted to 1 mL using 0.1 M PBS pH 7.4. In addition, H_2O_2 standard solutions at the concentration range of 0.001 to 1000 mM were prepared in 0.1 M PBS pH 7.4, as shown in Table 3.3, to determine a linear range and construct a calibration curve.

Table 3.3 Preparation of H_2O_2 standard solutions at different concentrations.

H_2O_2 (mM)	H_2O_2 stock standard solution		PBS (µL)
	Concentration (mM)	Volume (µL)	
0.001	0.1	10	990
0.005	0.1	50	950
0.01	0.1	100	900
0.05	0.1	500	500
0.1	20	5	995
0.5	20	25	975
1	20	50	950
10	20	500	500

H_2O_2 (mM)	H_2O_2 stock standard solution		PBS (µL)
	Concentration (mM)	Volume (µL)	
50	10,000	5	995
100	10,000	10	990
500	10,000	50	950
1,000	10,000	100	900

3.6 Electrode Optimization and Modification

3.6.1 CPE Optimization

Mineral oil, PDMS and graphite powder were mixed as carbon paste in a container until homogeneous texture was obtained before being screen-printed on an ePAD to fabricate WE and CE. The paste was prepared at different ratios (% w/w), whereas an oil phase was composed of the equal amounts of mineral oil and PDMS, as shown in Table 3.4. To compare these fabricated electrodes, the prepared ePADs at different ratios of paste were used to measure current of 10 mM $K_3Fe(CN)_6$ in 0.1 M KCl using CV with a potential range of -1.5 to 1.5 V and a scan rate of 50 mV s^{-1}.

Table 3.4 The ratios of oil phase and graphite powder to prepare CPEs. The total amount is 100 % w/w.

Oil		Graphite powder
Mineral oil	PDMS	
20	20	60
25	25	50
30	30	40

3.6.2 AgNPs and MWCNTs Modified CPE

Initially, AgNPs at a concentration of 10,000 ppm was used in the volume range of 0-1,000 µL with an interval of 200 µL. AgNPs were mixed with 0.5, 0.25 and 0.25 g of 1% w/w MWCNTs, mineral oil and PDMS, respectively, until homogeneous texture was obtained. Each CPE modified with AgNPs and MWCNTs (AgNPs-MWCNTs-CPE) was used to measure 20 mM H_2O_2 in 0.1 M PBS pH 7.4 using CV with the potential range of -1.5 to 1.5 V and a scan rate of 100 mV s^{-1}. After that, the amount of AgNPs which provided the highest current of 20 mM H_2O_2 was used to vary the amount of MWCNTs in the range of 0-2% w/w with an interval of 0.5% w/w. To modify CPE with MWCNTs, the MWCNTs were prepared separately in the range of 0-2% w/w, as shown in Table 3.5. Then, the CV measurements of the H_2O_2 were performed using the conditions similar to the optimization of AgNPs.

Table 3.5 Preparation of MWCNTs in the range of 0-2% w/w for electrode modification.

MWCNTs		Graphite power (g)
%	g	
0	0	1
0.5	0.0050	0.9950
1.0	0.0100	0.9900
1.5	0.0150	0.9850
2.0	0.0200	0.9800

3.6.3 Morphological Study

After the CPE was modified with AgNPs and MWCNTs (AgNPs-MWCNTs-CPE) which were screen-printed on the ePADs, the difference between the surface of a bared CPE and that of AgNPs-MWCNTs-CPE was investigated using a scanning electron microscope (SEM). The compositions of each electrode were characterized using energy-dispersive X-ray spectroscopy (EDX).

3.7 Electrochemical Study

In this work, oxalate was determined through the measurement of H_2O_2 produced from the enzymatic reaction. Therefore, 20 mM H_2O_2 in 0.1 M PBS pH 7.4 was used to study electrochemical performance of the AgNPs-MWCNTs-CPE using CV with the scan rate and potential ranges of 50 to 250 mV s^{-1} and 0 to -1.5 V, respectively. Peak current obtained from CV was measured and plotted with its scan rate and the square root of scan rate to determine the mass transfer process of H_2O_2 on the electrode surface.

3.8 Selection of Applied Potential

To select an applied potential for determination of H_2O_2 using amperometric detection, 20 mM H_2O_2 in 0.1 M PBS pH 7.4 was used to measure the peak current using applied potentials of -0.4, -0.6, -0.8, -0.9 and -1.2 V. To construct a hydrodynamic voltammogram, current signal of 20 mM H_2O_2 was divided by the background current (S/B) at the same potential and then the obtained S/B value was plotted versus its applied potential. The potential having the highest S/B ratio was used for amperometric measurements of H_2O_2.

3.9 Analytical Performance

3.9.1 Linearity and Calibration Curve

H_2O_2 standard solutions at the concentration range of 0.001 to 1,000 mM were used to study the linearity of this method. Current of each H_2O_2 concentration was measured using the optimized conditions and plotted versus the logarithmic of H_2O_2 concentration. The obtained linearity range of H_2O_2 concentration was used as a calibration curve for quantitative analysis of oxalate.

3.9.2 Limit of Detection (LOD) and Limit of Quantitation (LOQ)

The LOD and LOQ of this method was calculated from 3 and 10 times of SD divided by the slope of a calibration curve, as shown in Equations 3.1 and 3.2, respectively.

$$LOD = \frac{3\ SD}{slope} \tag{3.1}$$

$$LOQ = \frac{10\ SD}{slope} \tag{3.2}$$

3.10 Amperometric Detection of Oxalate Based on the Enzymatic Reaction

For the enzymatic reaction, 120 and 5 µL of sample solution and reagent B (containing OxOx and HRP) were pipetted into a reservoir of an ePAD. The mixed solution was incubated at room temperature for 5 min. After that, the produced H_2O_2 was measured for current using amperometric detection with the optimized conditions.

Part II Colorimetric Detection

3.11 Fabrication of Paper-Based Analytical Devices (PADs)

In this work, wax printing was selected for PADs fabrication. The array pattern of PADs was designed using CorelDraw X7 program. The pattern consisted of a hydrophilic area with a 7 mm diameter circle surrounded by a 4-point-thick line used as a wax hydrophobic barrier, as shown in Figure 3.4. The designed PADs were printed onto No.1 Whatman filter paper using a wax printer. The printed PADs were heated at 150 $^{\circ}$C for 1 min to melt the wax through the paper. The backside of the heated PADs was taped with an adhesive tape to prevent solution leakage and the front side was used for adding reagents and samples for reactions.

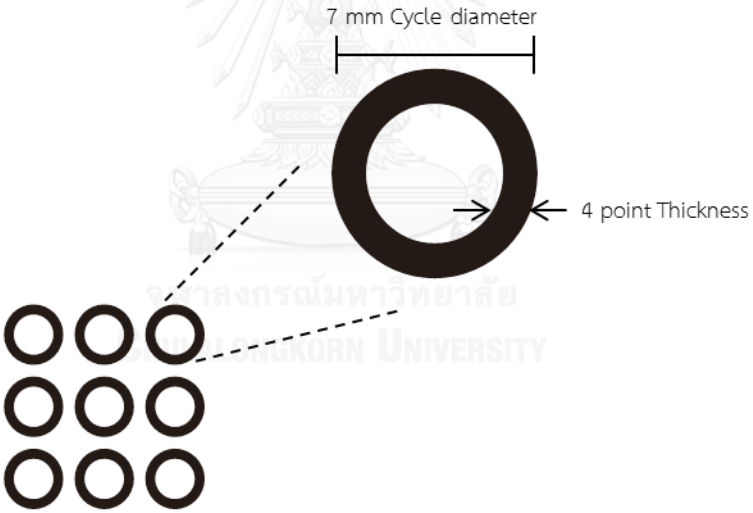

Figure 3.4 PADs designed using CorelDraw X7.

3.12 Solution Preparation

3.12.1 Phosphate Buffer Saline (PBS)

One tablet of PBS was dissolved in 200 mL of Milli-Q water to achieve 0.01 M PBS pH 7.4.

3.12.2 Oxalate Standard Solution

A stock standard solution of 1000 ppm oxalate was prepared in a volumemetric flask by dissolving 15.2 mg $Na_2C_2O_4$ in 10 mL of 0.01 M PBS pH 7.4. A series of oxalate standard solutions was prepared from the stock solution, as shown in Table 3.6.

Table 3.6 Preparation of oxalate standard solutions in 1 mL safe-lock tube.

Oxalate (ppm)	Volume of oxalate stock solution (µL)	Volume of PBS (µL)
0.5	0.5	999.5
1	1	999
5	5	995
10	10	990
20	20	980
30	30	970
40	40	960
50	50	950
100	100	900
200	200	800
300	300	700
500	500	500

3.12.3 Standard Solutions for Interference Study

Main components in human urine are composing of urea, AA, UA, CA, albumin (ALB) and Cr Stock standard solutions of all components for interference study were prepared in 10 mL volumetric flasks. All of stock standard solutions except for UA were prepared at a concentration of 1,000 ppm by dissolving 1 mg of each component in Milli-Q water. UA was prepared at 50,000 ppm by dissolving 50 mg UA in 0.5 mM NaOH.

3.12.4 Masking Reagents

A masking reagent containing 25 ppm $CuSO_4$ in 0.001 M HCl and a mixture solution of 0.12 M H_3BO_3 and 0.014 M NaOH was used to minimize the interfering effect of AA on colorimetric determination of oxalate using PADs.

3.12.4.1 $CuSO_4$ in HCl

A stock solution of 1 M HCl was prepared by pipetting 1.4 mL of conc. HCl into Milli-Q water in a 25 mL volumetric flask. HCl at a concentration of 0.001 M was prepared by pipetting 10 µL of the stock HCl solution into a 10 mL volumetric flask and Milli-Q water was used to make up the volume.

A stock solution of 500 ppm $CuSO_4$ was prepared in a 1.5 mL safe-lock tube by dissolving 1.26 mg $CuSO_4{\cdot}5H_2O$ in 0.001 M HCl. $CuSO_4$ at a concentration of 25 ppm $CuSO_4$ in 0.001 M HCl was prepared by pipetting 50 µL of the stock $CuSO_4$ solution into a 1.5 mL safe-lock tube. The total volume of 25 ppm $CuSO_4$ was adjusted to 1 mL using 0.001 M HCl.

3.12.4.2 A Mixture Solution of H_3BO_3 and NaOH

Stock solutions of 0.5 M H_3BO_3 and 0.1 M NaOH were prepared separately in 10 mL volumetric flasks by dissolving 309.15 mg of H_3BO_3 and 40 mg of NaOH in Milli-Q water.

A mixture solution of 0.12 M H_3BO_3 and 0.014 M NaOH was prepared in a 25 mL volumetric flask by diluting 6 mL of 0.5 M H_3BO_3 and 3.5 mL of 0.1 M NaOH in Milli-Q water.

3.12.5 Solutions for UV-Vis Spectrophotometry

A stock standard solution of 1,000 ppm oxalate was prepared in a volumetric flask by dissolving 15.2 mg $Na_2C_2O_4$ in 10 mL of Milli-Q water. A series of oxalate standard solutions was prepared from the stock solution, as shown in Table 3.7.

Table 3.7 Preparation of oxalate standard solutions in 1 mL safe-lock tube.

Oxalate (ppm)	Volume of oxalate stock solution (µL)	Milli-Q water (µL)
10	10	990
25	25	975
50	50	950
75	75	925
100	100	900

3.13 Colorimetric Detection of Oxalate Using PADs

For determination of oxalate, all solutions composing of reagent A, sample and reagent B were added into a reservoir of PADs using a micropipette. The mixed solution was incubated for 10 min at room temperature. After that, images of each reaction were taken using a DSLR D5300 Nikon camera. The camera was setup using a JPEG format, an A mode (aperture-priority auto), an aperture value of f/5, an exposure time of 1/800s, an ISO speed of 200, a focal length of 70 mm and a color representation in standard RGB (sRGB). A studio light box was used for imaging to prevent interfering of the external light. The color intensity of each reaction was measured using ImageJ. The schematic of experiments is shown in Figure 3.5. The difference of color intensity (ΔI), used for quantitative analysis, was calculated by subtraction between sample color intensity (I_{Sample}) and background color intensity ($I_{Background}$), as shown in Equation 3.3.

$$\Delta I = I_{Sample} - I_{Background} \quad (3.3)$$

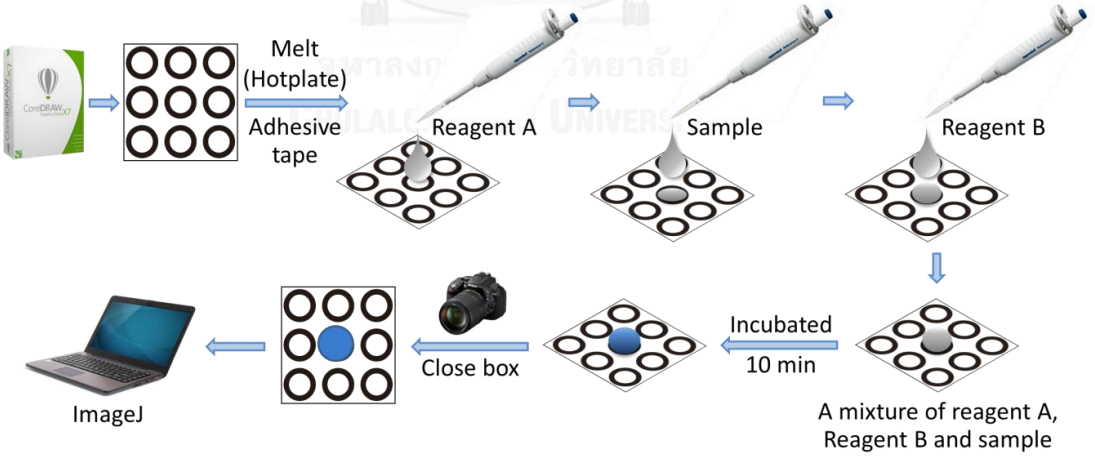

Figure 3.5 Schematic representation of experimental procedure for determination of oxalate using PADs.

3.14 Optimization of Experimental Parameters for Determination of Oxalate Using PADs

3.14.1 The Amounts of Reagents A and B

For colorimetric detection of oxalate based on the enzymatic reaction, the amounts of reagents A and B were optimized to obtain the highest color intensity. The volume of reagents A and B was varied in the ranges of 5-30 µL and 1-5 µL, respectively, to react with 300 ppm oxalate standard solution. The color intensity from the reaction was measured at 10 min of the reaction time.

3.14.2 The Reaction Time

To determine the suitable reaction time of the enzymatic reaction, the color intensity from the reaction was measured every 5 min for 60 min to investigate the reaction time which provided the highest color intensity.

3.14.3 pH of PBS Buffer

For determination of oxalate using the oxalate kit, pH of urine samples should be between 5.0 - 7.0 as recommended from the oxalate kit manual. To study effect of pH, 0.01 M PBS was adjusted to pH 5.0, 5.5, 6.0, 6.5 and 7.0 using 1 M HCl. After that, the adjusted PBS was used to prepare 40 ppm oxalate and then the solutions were used to react with reagents A and B on PADs. The color intensity of the reaction was measured at 10 min of the reaction time.

3.15 Interference Study

Effect of the main components (urea, AA, UA, CA, Cr and ALB) in urine on the colorimetric detection of oxalate based on the enzymatic reaction was studied. The normal levels of each component in urine, as shown in Table 3.8, were prepared in 0.01 M PBS pH 7.4 containing 40 ppm oxalate. The percentage difference (%difference) of ΔI was used to indicate which component interfered the determination of oxalate based on the colorimetric detection.

To calculate %difference of ΔI, the obtained ΔI of 40 ppm oxalate containing each component ($\Delta I_{Mixture}$) was compared with that of 40 ppm oxalate standard solution ($\Delta I_{Oxalate}$), as shown in Equation 3.4. The component giving the %difference of ΔI higher 5% was considered as an interfering component that affected the oxalate detection.

$$\%\text{Difference} = \frac{(\Delta I_{Oxalate} - \Delta I_{Mixture})}{\Delta I_{Oxalate}} \times 100 \qquad (3.4)$$

Table 3.8 The normal levels of main components in human urine [4, 63-67].

Components	Normal level (ppm)
Urea	20,000
Ascorbic acid (AA)	600
Uric acid (UA)	250
Citric acid (CA)	321
Creatinine (Cr)	250
Albumin (ALB)	30

3.16 Analytical Performance

3.16.1 Linearity and Calibration Curve

To investigate a linear relationship between oxalate concentration and ΔI, oxalate concentrations in the range of 5 to 1,000 ppm were studied using the optimized conditions. Each oxalate concentration was mixed with 50 µL of 25 ppm $CuSO_4$, 450 µL of H_3BO_3 (0.12 M) - NaOH (0.014 M) to minimize the interfering effect of AA for colorimetric detection of oxalate based on the enzymatic reaction. The total volume of each concentration was adjusted to 1 mL in a safe-lock tubes using 0.01 mM PBS pH 7.4. The obtained ΔI values were plotted versus concentration. A linear range of the graph was used as a calibration curve. A linear equation from the calibration curve was used for quantitative analysis of oxalate.

3.16.2 Limit of Detection (LOD) and Limit of Quantitation (LOQ)

To calculate LOD and LOQ, 3 and 10 times of standard deviation (SD) divided by the slope of a calibration curve were used, respectively, as shown in Equations 3.5 and 3.6:

$$LOD = \frac{3SD}{slope} \quad (3.5)$$

$$LOQ = \frac{10SD}{slope} \quad (3.6)$$

3.16.3 Accuracy

The percent recovery (%recovery) of added oxalate standard solutions in urine samples was used to determine accuracy of the method. As shown in Table 3.9, oxalate concentrations of 5, 15 and 30 ppm, 25 ppm $CuSO_4$ and H_3BO_3 (0.12 M) - NaOH (0.014 M) were added in urine samples. The total volume of each sample was adjusted to 1 mL in a safe-lock tube using 0.01 M PBS pH 7.4.

Table 3.9 The volume of each solution for urine sample preparation to determine accuracy of the method.

Sample (µL)	Added oxalate (ppm)	Stock oxalate standard solution (µL)	25 ppm $CuSO_4$ (µL)	0.012 M H_3BO_3 (µL)	PBS (µL)
200	5	5	50	450	295
200	15	15	50	450	285
200	30	30	50	450	270

For urine samples without added standard oxalate solutions, urine samples (200 µL) were prepared by adding the masking reagent (the same volumes as shown in Table 3.9) and 300 µL of 0.01 M PBS pH 7.4.

To calculate %recovery, the obtained ΔI values of standard oxalate solutions ($\Delta I_{Oxalate\ standard}$), urine samples ($\Delta I_{Sample}$) and urine samples added with oxalate standard solution ($\Delta I_{Spiked\ sample}$) were used to calculate using Equation 3.7:

$$\%Recovery = \frac{\Delta I_{Spiked\ sample} - \Delta I_{Sample}}{\Delta I_{Oxalate\ standard}} \times 100 \qquad (3.7)$$

3.16.4 Precision

Precision of the method for oxalate detection in urine samples was determined as intra-day and inter-day precisions.

For intra-day precision, 5, 15 and 30 ppm oxalate standard solutions were added in urine containing the masking reagent, as shown in Table 3.10. Each reaction was incubated at room temperature for 30 min. After that, each solution was pipetted to react with reagents A and B using the optimized conditions. The observed color intensity was measured at 10 min of the reaction time. Each solution was prepared and measured for 11 replicates in a day.

For inter-day precision, each solution (the same as used for intra-day precision) was prepared and measured every day for 3 days.

The percentage of relative standard deviation (%RSD) of each reaction was calculated using Equation 3.8 to determine the precisions.

$$\%RSD = \frac{SD}{\bar{x}} x100 \quad (3.8)$$

where SD is standard deviation and $\bar{x}$ is averaged color intensity.

Table 3.10 Solution preparation to investigate intra-day and inter-day precisions of this method on oxalate detection using PADs. The total volume was adjusted to 1 mL using 0.01 M PBS pH 7.4.

Sample (µL)	Oxalate		PBS (µL)	25 ppm $CuSO_4$ (µL)	H_3BO_3-NaOH (µL)
	Spiked (ppm)	Stock 1,000 ppm (µL)			
200	0	0	300	50	450
200	5	5	295	50	450
200	15	15	285	50	450
200	30	30	270	50	450

3.17 Comparison of PADs and Standard Method for Determination of Oxalate in Urine.

Urine samples were obtained from the Faculty of Medicine, Chulalongkorn University. The amount of oxalate in urine samples obtained from this method and UV-Vis spectrophotometry a standard method was compared using the student t-test at a 95% confident interval.

3.17.1 Determination of Oxalate in Urine Samples Using PADs

Samples were prepared using 200 µL urine, 300 µL of 0.01 M PBS pH 7.4 and 500 µL of the masking reagent including 50 µL of 25 ppm $CuSO_4$ and 450 µL of H_3BO_3 (0.12 M) - NaOH (0.014 M). The samples were incubated at room temperature for 30 min to minimize the interfering effect of AA. After that, 5 µL samples were pipetted to react with reagents A and B in the reservoirs of a PAD. The obtained ΔI values were converted to oxalate concentrations using a linear calibration curve.

3.17.2 Determination of Oxalate in Urine Using an Oxalate Kit and UV-Vis Spectrophotometry

For sample preparation, the same urine samples as used for the PADs were 2-fold diluted with a sample diluent obtained from an oxalate kit. The pH of each diluted samples was adjusted to 5.0 - 7.0 according to the oxalate kit manual using 1.0 M HCl or 1.0 M NaOH. The diluted samples were pipetted into sample purifier tubes and mixed approximately for 5 min. After that, the tubes were centrifuged for 5 min at 3,000 rpm to separate supernatant and solid matters.

The oxalate kit was used to determine oxalate in urine sample based on the enzymatic reaction using a UV-Vis spectrophotometry. To construct a calibration curve, 500 µL of reagent A, 25 µL of oxalate at the concentration range of 10 to 100 ppm and 50 µL of reagent B were pipetted in cuvettes, respectively, using a reagent blank as a background. The mixed solutions were incubated at room temperature for 5 min and then measured absorbance at a wavelength of 590 nm. The same condition was used absorbance measurement of urine samples. The absorbance (A) values from each urine samples was converted to oxalate concentrations using a linear calibration curve.

3.17.3 Comparison of Two Methods Using the Student t-test and the Linear Regression Analysis.

The reliability of PADs for determination of oxalate in urine was compared with UV-Vis spectrophotometry as a standard method using the student t-test at a 95% confident interval. Furthermore, a graph of the oxalate concentrations in urine obtained from PADs versus those obtained from UV-Vis spectrophotometry was also used to determine the accuracy of PADs for determination of oxalate in urine.

CHAPTER IV
RESULTS AND DISSCUSION

Part I Electrochemical Detection of Oxalate

The determination of oxalate using electrochemical detection was performed based on the enzymatic reaction. For the enzymatic reaction, oxalate in the solution reacted with OxOx in the presence of O_2 to produce H_2O_2, as shown in Figure 4.1. The amount of H_2O_2 was related to the amount of oxalate in the solution. Therefore, the produced H_2O_2 was used to measure the amount of oxalate through the reduction of H_2O_2. The obtained current from the reduction of H_2O_2 was used to calculate the amount of oxalate using the linear equation of a calibration curve.

$$\text{Oxalate} + O_2 \xrightarrow{\text{Oxalate Oxidase (OxOx)}} 2CO_2 + H_2O_2$$

$$H_2O_2 + 2H^+ + 2e^- \longrightarrow 2H_2O$$

Figure 4.1 The enzymatic reaction of oxalate for the electrochemical detection of oxalate.

4.1 Electrode Optimization and Modification

4.1.1 CPE Optimization

Normally, CPE consisted of mineral oil and graphite powder. In this work, PDMS was mixed with mineral oil and graphite powder to stabilize CPEs on ePADs because the outer surface of CPEs without PDMS could be lost when the solution in the reservoir was removed [68]. CV was used to measure current of 10 mM $K_3Fe(CN)_6$ in 0.1 M KCl using different component ratios of electrode fabrication. The components of CPEs were varied to obtain the highest current. As shown in Figure 4.2, the peak current of 10 mM $K_3Fe(CN)_6$ in 0.1 M KCl was increased when

increasing the ratio of graphite powder because of the conductivity of graphite powder. If the amount of oil phase (mineral oil and PDMS) used to fabricate CPEs was lower than 30% w/w (oil : graphite powder), the obtained carbon paste was not be able to screen-print on the filter paper due to its crumbly texture. Also, the 70% w/w (oil : graphite powder), carbon paste was not be able to screen-print on the filter paper because the texture was relatively liquid.

Although peak currents obtained from 50% and 60% w/w (oil: graphite powder) were slightly different, 50% w/w (oil: graphite powder) was used because it was easier to screen-print on paper and provided slightly higher peak current. Therefore, the CPE composition of 50% w/w (oil: graphite powder) was used to mix with AgNPs and MWCNTs for electrode fabrication for the measurements of H_2O_2 to determine the amount of oxalate based on the enzymatic reaction.

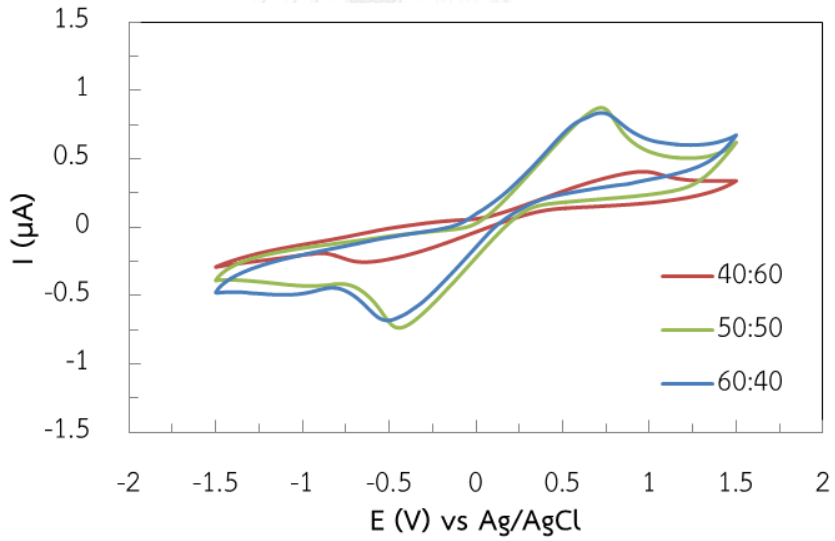

Figure 4.2 Cyclic voltammograms of 10 mM $K_3Fe(CN)_6$ in 0.1 M KCl obtained from different CPEs fabricated using different ratios of mineral oil, PDMS and graphite powder. CV measurements were performed using the potential range of -1.5 to 1.5 V and a scan rate of 50 mV s^{-1}.

4.1.2 AgNPs and MWCNTs Modified CPE

Initially, 1% w/w MWCNTs was used to optimize the amount of 10,000 ppm AgNPs for WE modification. Various amounts of AgNPs were mixed with the equal amount of 1% w/w MWCNTs, mineral oil and PDMS. After that, the mixed paste with different amounts of AgNPs was screen-printed onto an ePAD to fabricate a WE. CV was used to measure current of 20 mM H_2O_2 using the electrode fabricated from the different amounts of AgNPs. The cathodic peak currents (i_{pc}) obtained from different compositions of CPEs were used to plot with the amount of AgNPs, which was used to modify the CPE, as shown in Figure 4.3 (a). The current increased when increasing the amount of AgNPs because of the higher electrode surface. However, the current decreased when using the amount of 10,000 ppm AgNPs higher than 400 µL. This was because AgNPs at higher concentrations could aggregate, which decreased the electrode surface area [69]. Therefore, 400 µL of 10,000 ppm AgNPs was used as an optimized amount of AgNPs for WE modification.

After that, the optimized amount of AgNPs was used to optimize the amount of MWCNTs. The fabricated ePADs using different % w/w values of MWCNTs for modification of WE were used to measure current of 20 mM H_2O_2 using CV. The obtained i_{pc} of 20 mM H_2O_2 was plotted with the amount of MWCNTs, as shown in Figure 4.3 (b). The current increased when increasing the amount of MWCNTs because MWCNTs could enhance the surface area of the electrode [18, 21]. If the amount of MWCNTs was higher than 1% w/w, the current decreased because the higher electrode surface area could also result in higher background current [70, 71]. Therefore, the optimum amount of MWCNTs was found to be 1% w/w, providing the highest current of 20 mM H_2O_2.

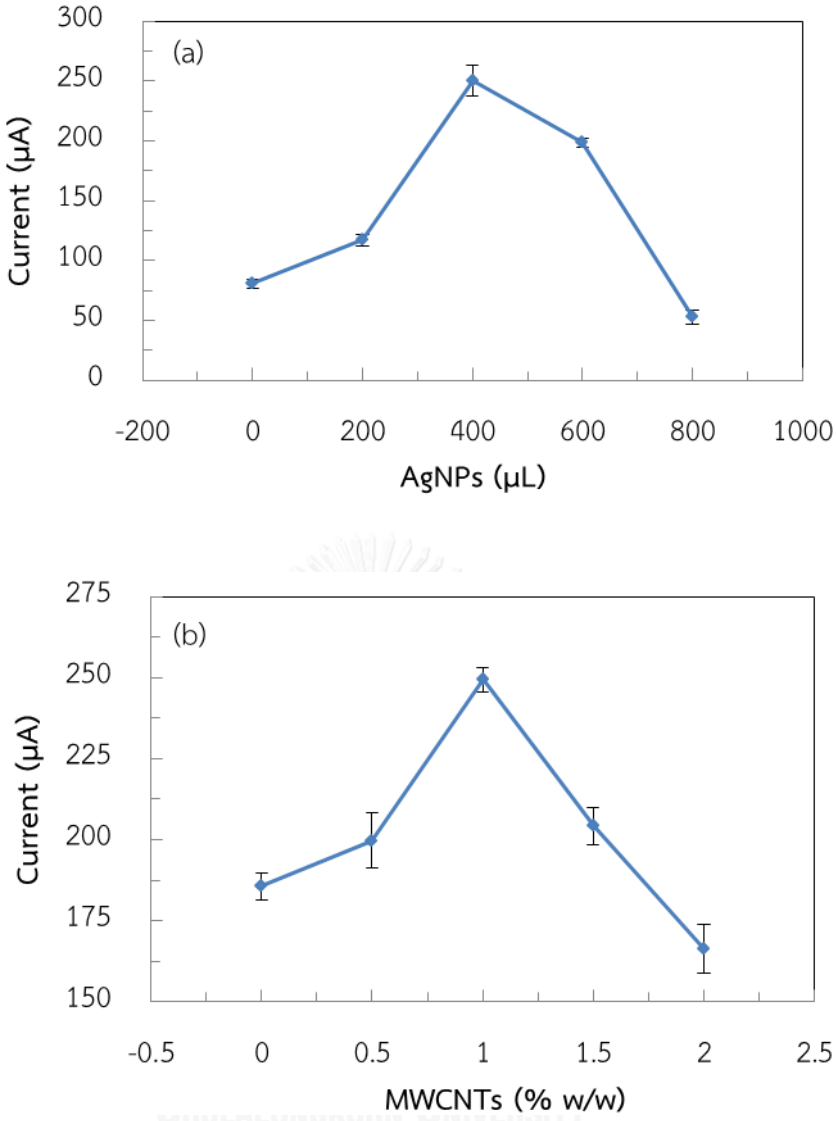

Figure 4.3 Optimization of the amounts of AgNPs (a) and MWCNTs (b). The current of 20 mM H_2O_2 in 0.1 M PBS pH 7.4 was measured using CV with the optimized conditions as shown in Figure 4.2.

Therefore, 400 µL of 10,000 ppm AgNPs and 1 % w/w MWCNTs were used to mix with 50 % w/w (oil : graphite powder) carbon paste before being screened on filter paper as a WE which is called AgNPs-MWCNTs-CPE.

Cyclic voltammograms of a bare CPE, AgNPs-CPE, MWCNTs-CPE and AgNPs-MWCNTs-CPE were compared in Figure 4.4. As expected, the highest current of 20 mM H_2O_2 was obtained when using the AgNPs-MWCNTs-CPE as a WE. Therefore, AgNPs-MWCNTs-CPE was used in this work for determination of oxalate through the measurement of H_2O_2, which was generated from the enzymatic reaction. Electrochemical measurements of H_2O_2 could be performed using either oxidation or reduction of H_2O_2. However, in previous work [71], many components, such as ascorbic acid, uric acid and dopamine could interfere the measurements of H_2O_2 from the oxidation reaction. To avoid this problem, only reduction reaction of H_2O_2 was considered in this work.

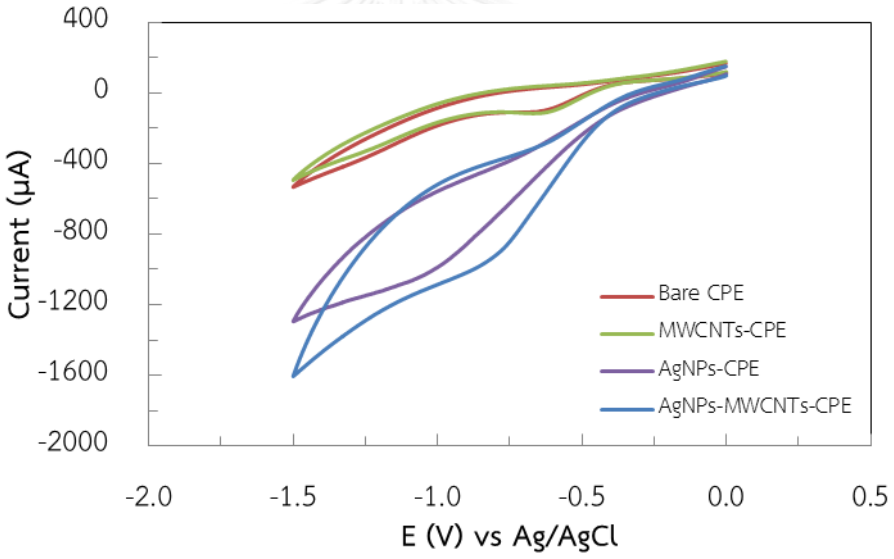

Figure 4.4 A comparison of cyclic voltammograms obtained from a bared CPE and modified CPEs.

4.2 Electrode Characterization

4.2.1 Morphological Study

The surface morphology of a WE was studied using SEM. Figure 4.5 (a) shows the smooth surface of a bare CPE, whereas the rough surface of AgNPs-MWCNTs-CPE was observed due to the distribution of AgNPs and MWCNTs, as shown in Figure 4.5 (b).

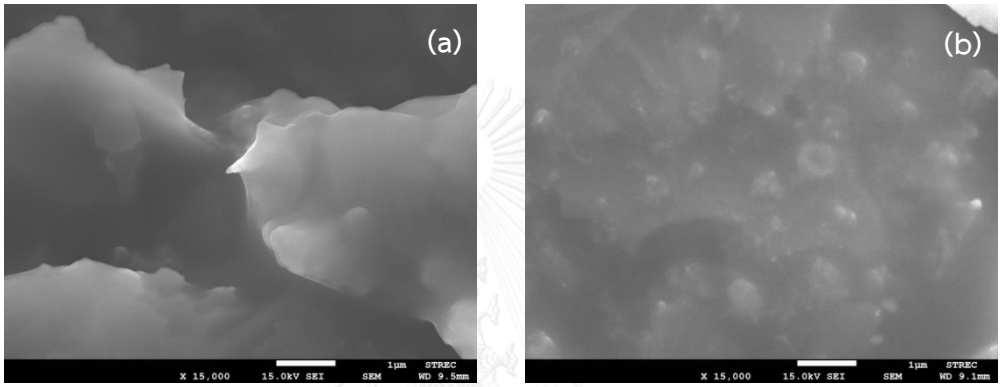

Figure 4.5 SEM images of (a) a bare CPE and (b) an AgNPs-MWCNTs-CPE.

To confirm that AgNPs were contained in the AgNPs-MWCNTs-CPE, EDX was used to detect all elements in a bare CPE (Figure 4.6 (a)) compared with an AgNPs-MWCNTs-CPE (Figure 4.6 (b). As shown in Figure 4.6 (c), a bare CPE composed of 89.59, 8.58, 0.07 and 1.76% w/w of C, O, Al and Si, respectively. For the AgNPs-MWCNTs-CPE, the amounts of C, O, Na, Al, Si and Ag were 79.87, 12.63, 5.41, 1.12, 0.76 and 0.21% w/w, respectively, as shown in Figure 4.6 (d). The results from EDX confirmed that AgNPs were contained on the surface of AgNPs-MWCNTs-CPE.

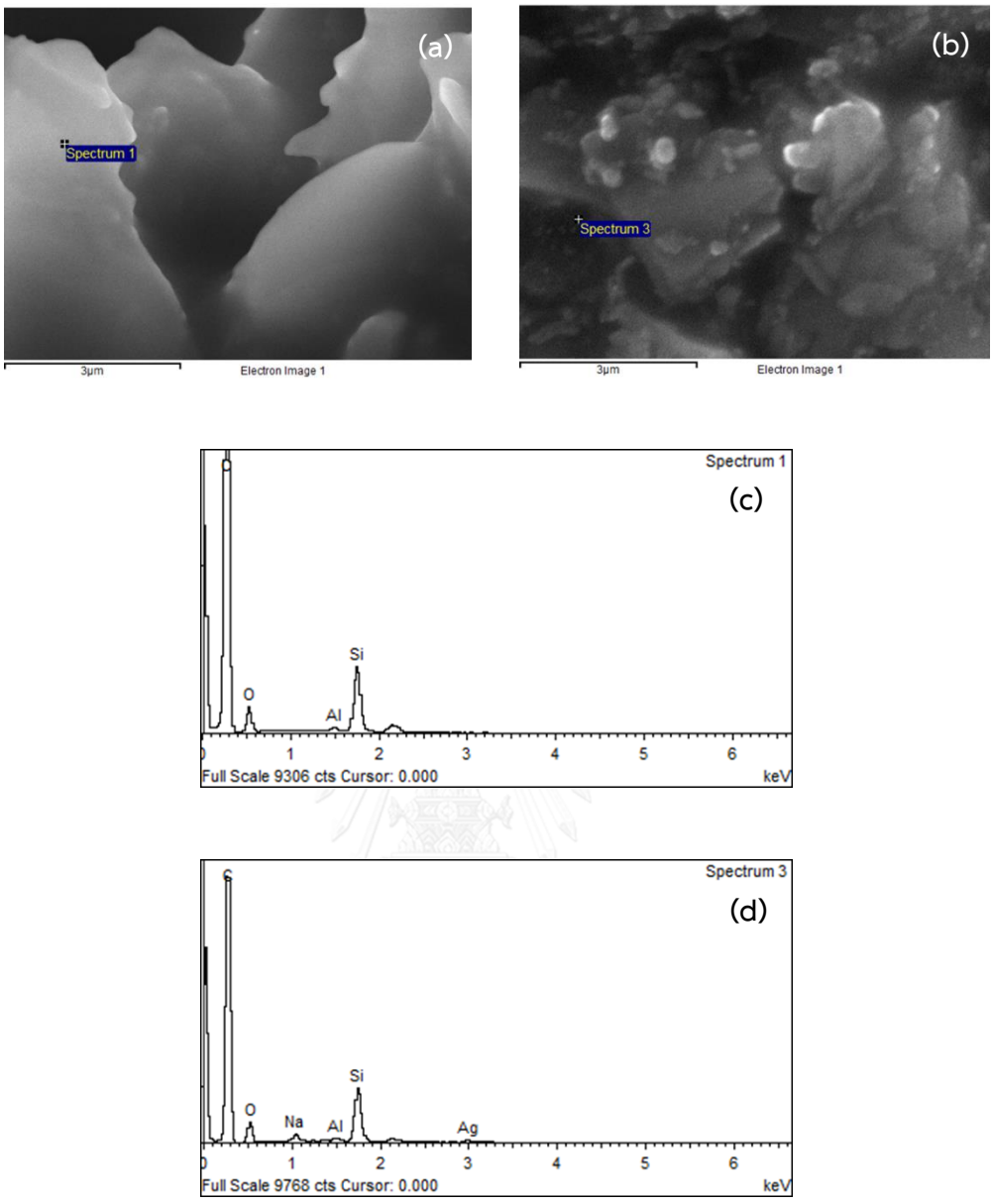

Figure 4.6 EDX analysis of (c) a bare CPE and (d) a AgNPs-MWCNTs-CPE from the SEM images of (a) a bare CPE and (b) a AgNPs-MWCNTs-CPE.

4.2.2 Electrochemical Study

In this work, the amount of oxalate was determined through electrochemical measurements of H_2O_2. Therefore, H_2O_2 was used to study the electrochemical behavior occurring at the surface of the modified CPE. Scan rate was an important parameter to study the mass transfer process of H_2O_2 between bulk solution and the electrode surface. The mass transfer process indicates that current is from faradaic or non-faradaic process. Cyclic voltammograms of H_2O_2 at the scan rate range of 50 to 250 mV s^{-1} are shown in Figure 4.7 (a). The obtained anodic peak current was plotted with its scan rate and the square root of scan rate, as shown in Figures 4.7 (b) and (c), respectively. The graph between current and the square root of scan rate was more linear when compared to the graph between current and scan rate. Therefore, the mass transfer process was considered as a diffusion-controlled process. As shown in Figure 4.7 (a), a peak shift was observed due to the minor effect of an adsorption-controlled process.

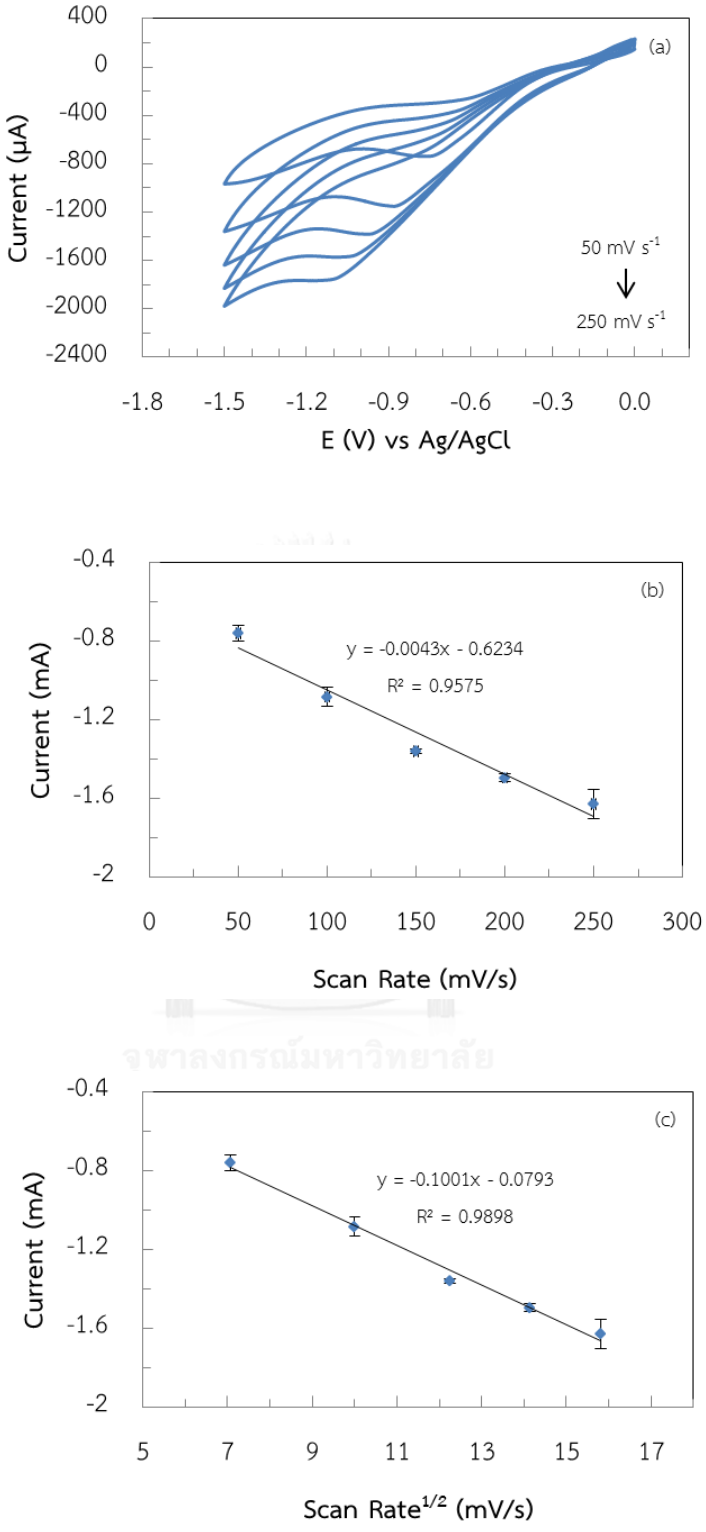

Figure 4.7 (a) Cyclic voltammograms of 20 mM H_2O_2 in 0.1 M PBS pH 7.4 using the scan rate range of 50 to 250 mV s^{-1}. Plots of peak current with scan rate (b) and the square root of scan rate (c).

4.3 Selection of Applied Potential

To determine an applied potential for amperometric detection of oxalate, a hydrodynamic voltammogram was constructed to select the optimum potential. As shown in Figure 4.8 (a), the reduction current of 20 mM H_2O_2 was increased when increasing an applied potential in the range of -0.4 to -1.2 V. The current of H_2O_2 was divided by the background current of 0.1 M PBS pH 7.4 (at the same potential) to obtain S/B ratios, which were plotted versus applied potential, as shown in Figure 4.8 (b). The S/B ratios were increased when increasing the applied potential from -0.4 to -0.6 V and decreased when using the applied potential more negative than -0.6 V. This was because the use of high applied potentials could increase the background current and the reduction of oxygen could occur at the potentials more negative than -0.5 V [72]. Therefore, an applied potential of -0.6 V was used for amperometric detection of oxalate using ePADs based on the enzymatic reaction.

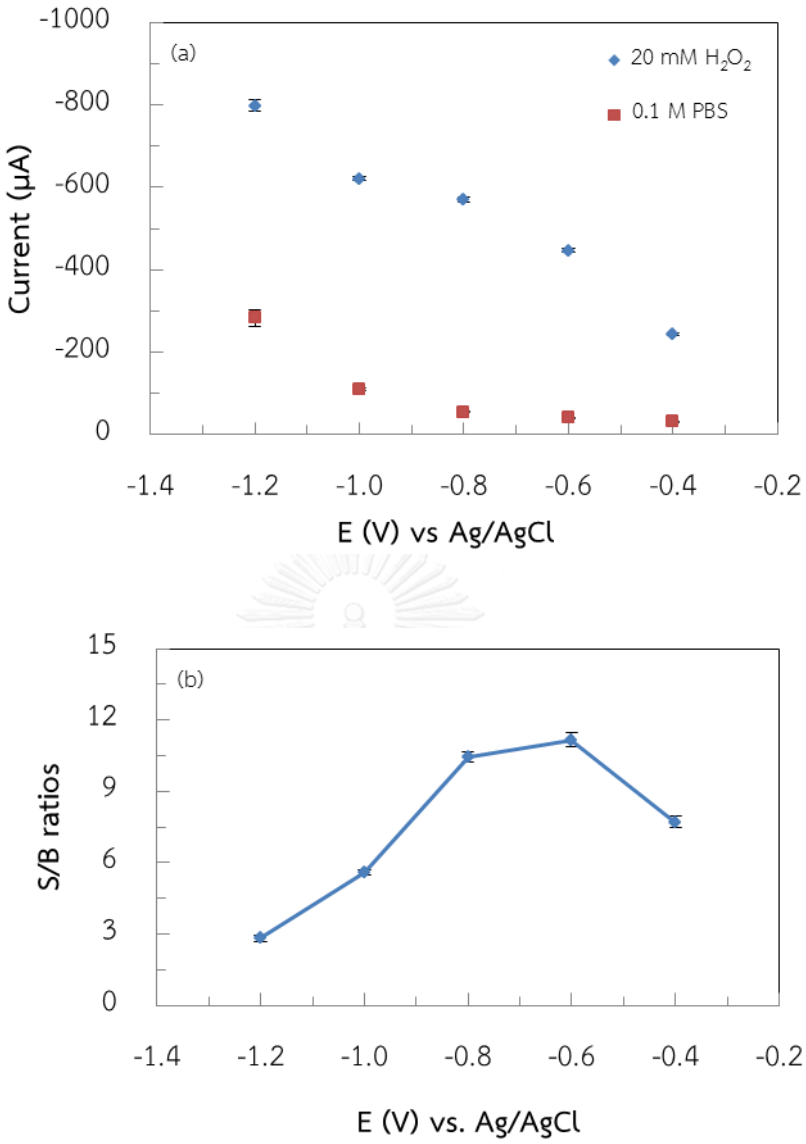

Figure 4.8 (a) Current signal from 20 mM H_2O_2 and 0.1 M PBS pH 7.4 when using applied potentials in the range of -0.3 to 1.2 V. (b) A hydrodynamic voltammogram plotted using S/B ratio as a function of applied potential.

4.4 Analytical Performance

4.4.1 Linearity and Calibration Curve

For quantitative analysis, linearity was studied using H_2O_2 standard solution at the concentration range of 0.001 to 1000 mM. A potential of -0.6 V was used to apply for the amperometric measurement of H_2O_2. The obtained current from amperometric detection of H_2O_2 was plotted with the logarithm of each concentration, as shown in Figure 4.9 (a), providing two linear ranges. The first linear range was observed in the concentration range of 0.05 - 10 mM H_2O_2 with a logarithmic equation of y = -30.79ln(x) - 191.83 and a correlation coefficient of 0.9973. The second linear range was observed in the concentration range of 10 - 1,000 mM H_2O_2 with a logarithmic equation of y = -325.8ln(x) - 566.31 and a correlation coefficient of 0.9864.

According to the reaction in Figure 4.1, the amount of H_2O_2 produced from the enzymatic reaction corresponds to the amount of oxalate in the solution. From the normal level of oxalate (40 ppm) in urine of healthy people, this oxalate concentration should produce H_2O_2 concentration which is in the first linear range. Therefore, the first linearity was used as a calibration curve, as shown in Figure 4.9 (b), in this work. Amperometric response of each H_2O_2 concentration shown in the calibration curve is shown in Figure 4.9 (c).

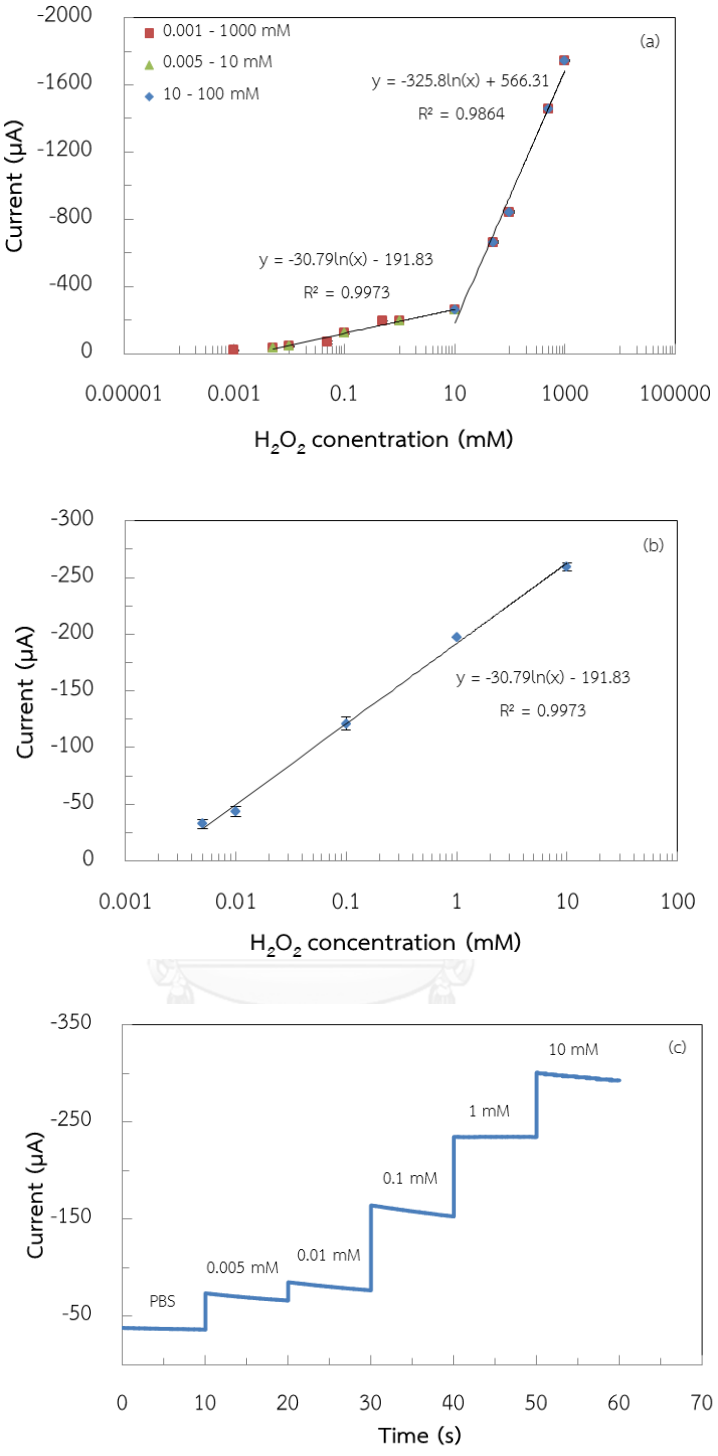

Figure 4.9 (a) The current signal of H_2O_2 at the concentration range of 0.001 to 1,000 mM. (b) A calibration curve which was from the first linear range of the plot in (a). (c) Amperometric response of H_2O_2 at the concentrations shown in the calibration curve in (b).

4.4.2 Limit of Detection (LOD) and Limit of Quantitation (LOQ)

From the calibration curve, LOD and LOQ for determination of H_2O_2 were calculated from 3 and 10 times of SD divided by the slope of calibration curve and found to be approximately 0.02 and 0.08 ppm, respectively.

4.5 Determination of Oxalate Based on the Enzymatic Reaction

For determination of oxalate based on the enzymatic reaction, 120 µL of 40 ppm oxalate standard solution and 5 µL of reagent B were pipetted into the reservoir of an ePAD. The mixed solution was incubated at room temperature for 5 min. Oxalate in the solution was reacted with OxOx in the reagent B to produce H_2O_2. The amount of the produced H_2O_2 was measured using amperometric detection with an applied potential of -0.6 V. The current obtained from the produced H_2O_2 was corresponded to the amount of oxalate in the solution.

However, it was found that relatively low current signal from the reaction from the amperometric measurement was observed. This could be because reagent B consisted of OxOx and HRP. Therefore, the H_2O_2 generated from the enzymatic reaction between OxOx and oxalate was simultaneously reduced by HRP to produce H_2O and the oxidized form of HRP as below [73]:

$$H_2O_2 + HRP_{red} \rightarrow H_2O + HRP_{ox}$$

Accordingly, there was no H_2O_2 to be measured by the AgNPs-MWCNTs-CPE.

Since the AgNPs-MWCNTs-CPE was fabricated and optimized to detect H_2O_2, it might not be suitable to amperometrically measure the oxidized form of HRP. Therefore, pure OxOx should be used for this measurement to produce H_2O_2. However, pure OxOx is not commercially available. Accordlingly, determination of oxalate based on PADs was changed from electrochemical detection to colorimetric detection. Therefore, the determination of oxalate using PADs coupled with

colorimetric detection was developed in this work instead of electrochemical detection.

Part II Colorimetric Detection of Oxalate

For colorimetric detection of oxalate based on the enzymatic reaction using PADs, oxalate reacted with OxOx enzyme in the presence of O_2 to produce CO_2 and H_2O_2. After that, the produced H_2O_2 reacted with MBTH and DMAB in the presence of HRP to produce an indamine dye as a blue color. All of the reactions are shown in Figure 4.10. The color intensity of the indamine dye corresponded to the amount of oxalate in the solution. Therefore, the color intensity was measured using ImageJ and used in quantitative analysis of oxalate in samples.

$$\text{Oxalate} + O_2 \xrightarrow{\text{Oxalate Oxidase (OxOx)}} 2CO_2 + H_2O_2$$

$$H_2O_2 + \text{MBTH} + \text{DMAB} \xrightarrow{\text{Horseradish peroxidase (HRP)}} \text{Indamine Dye} + H_2O$$

Figure 4.10 The enzymatic reactions for colorimetric detection of oxalate.

4.6 Optimization of Experimental Parameters for Colorimetric Determination of Oxalate Using PADs

4.6.1 The Amounts of Reagents A and B

From oxalate kit, 3.2 mM DMAB and 0.22 mM MBTH were mixed as a reagent A and 3,000 u L^{-1} OxOx was mixed with 100 u L^{-1} HRP as a reagent B. The volume of each reagent was varied to obtain the highest color intensity of the colorimetric detection. For optimization of the volumes of reagents A and B, 5 µL of 300 ppm oxalate standard solution was used to react with reagents A and B because it is a high concentration level of oxalate found in patients. The total volume in the reservoir of PADs was adjusted to 40 µL using 0.01 M PBS pH 7.4. A photograph of each reaction was taken at 10 min of the reaction time in a studio light box to prevent the external light and then measured the color intensity using ImageJ program.

Initially, the volume of reagent A was fixed at 30 µL to react with reagent B in the volume range of 0 to 5 µL. As shown in Figure 4.11 (a), the obtained ΔI was increased when increasing the volume of reagent B from 0 to 2 µL because the produced H_2O_2 were increased when increasing the amount of OxOx, which was mixed as a reagent B. The higher amount of the produced H_2O_2 reaching with DMAB and MBTH in reagent B resulted in the increase of indamine dye color intensity. After that, the ΔI was relatively constant due to the excess amount of OxOx in the reagent B. The highest ΔI was obtained when using 5 µL of reagent B, which corresponded to 3×10^{-3} u L^{-1} OxOx and 1×10^{-4} u L^{-1} HRP. Therefore, 5 µL was used as an optimized volume of reagent B.

To optimize the volume of reagent A, 5 µL of reagent B was used and the volume of reagent A was varied in the range of 0 to 30 µL. Similar to reagent B, the ΔI was increased when increasing the volume of reagent A, as shown in Figure 4.11 (b). The H_2O_2 produced from the enzymatic reaction reacted with the different amounts of MBTH and DMAB, which were mixed as the reagent A, to produce the indamine dye as a blue color. Therefore the color intensity was increased when increasing the amount of reagent A. However, the obtained ΔI tended to slightly increase when using the volume of reagent A more than 30 µL. Since the total volume was fixed at 40 µL and 5 µL of each reagent B and sample was used, the highest volume of reagent A was not over 30 µL. Thus, 30 µL was selected as an optimized volume of reagent A, which corresponded to 2.4 mM DMAB and 0.0176 mM MBTH.

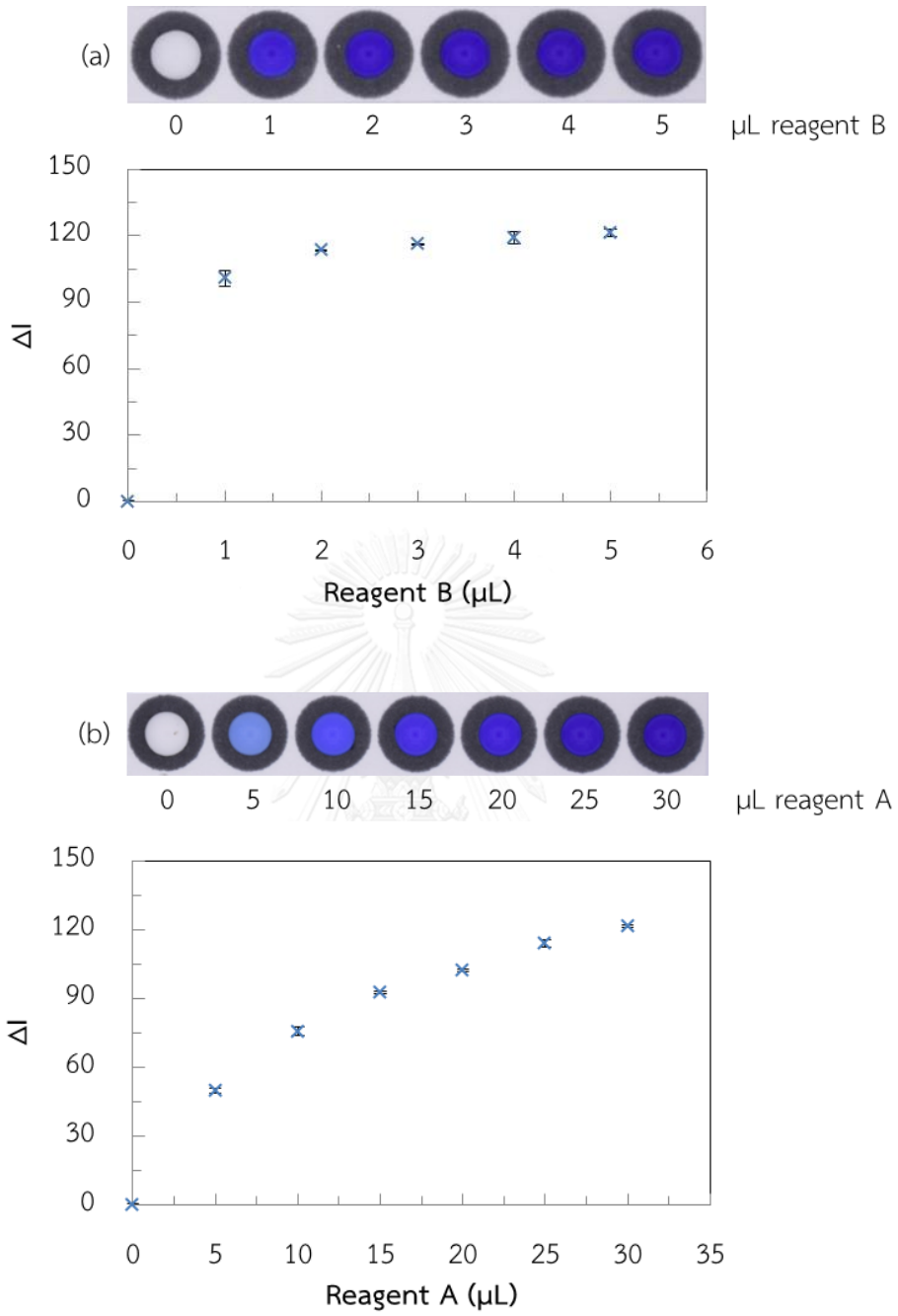

Figure 4.11 Optimization of the amounts of reagents B (a) and A (b).

4.6.2 The Reaction Time

For colorimetric detection of oxalate based on the enzymatic reaction, the color intensity from the reaction is based on the reaction time. Therefore, the reaction time was optimized to obtain the highest color intensity. Oxalate standard solutions at concentrations of 5, 10, 25 and 250 ppm were used in order to cover the oxalate concentration found in urine of healthy people and kidney stone patients.

After mixing the optimized amounts of reagents A (30 µL) and B (5 µL) with oxalate solutions in the reservoirs of PADs, photographs of each reaction were taken every 10 min for 60 min. The observed color was shown in Figure 4.12 (a). The color intensity of each reservoir was measured using ImageJ program to calculate ΔI. The relationship between the obtained ΔI values at different oxalate concentrations and the reaction time was shown in Figure 4.12 (b). The ΔI values were increased when increasing the reaction time from 1 to 10 min. After that, the obtained ΔI values were slightly decreased, especially at high concentrations (≥50 ppm). This was because the solutions were dried and the color intensity was faded. Therefore, 10 min was selected as an optimized reaction time in this work.

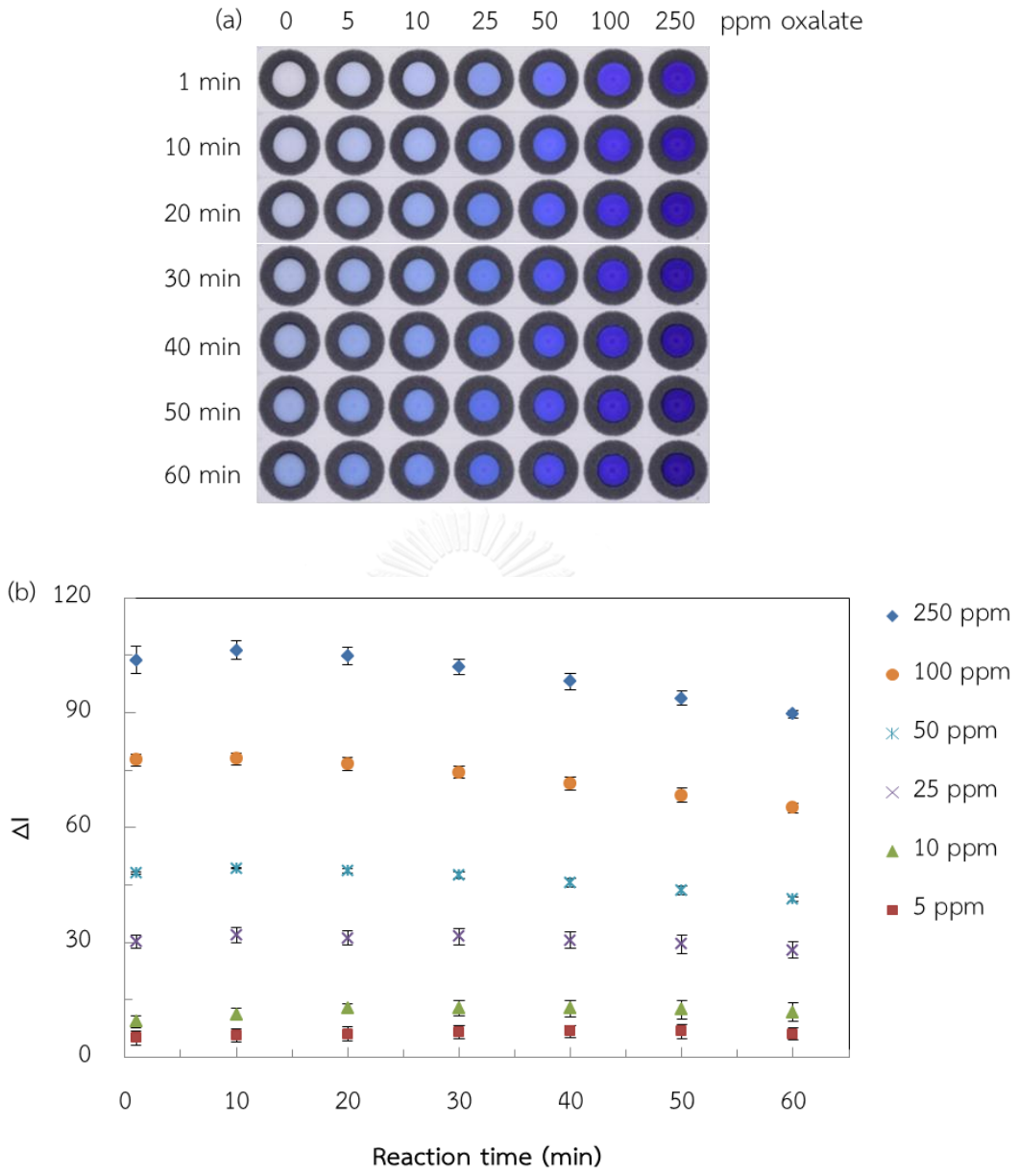

Figure 4.12 The observed color from each reaction time (a) and the relationship between ΔI and reaction time (b) when using different oxalate concentrations.

4.6.3 pH of PBS Buffer

To determine a suitable pH, 40 ppm oxalate standard solution was prepared using different pH values of PBS buffer. Although the observed color intensities from each pH , as shown in Figure 4.13, were not significantly different, the highest ΔI values of approximately 46 were obtained at pH 6.5-7.4, which corresponded to the recommended pH from the oxalate kit manual. Therefore, pH 7.4 was selected as an optimized pH because it was easy to prepare PBS.

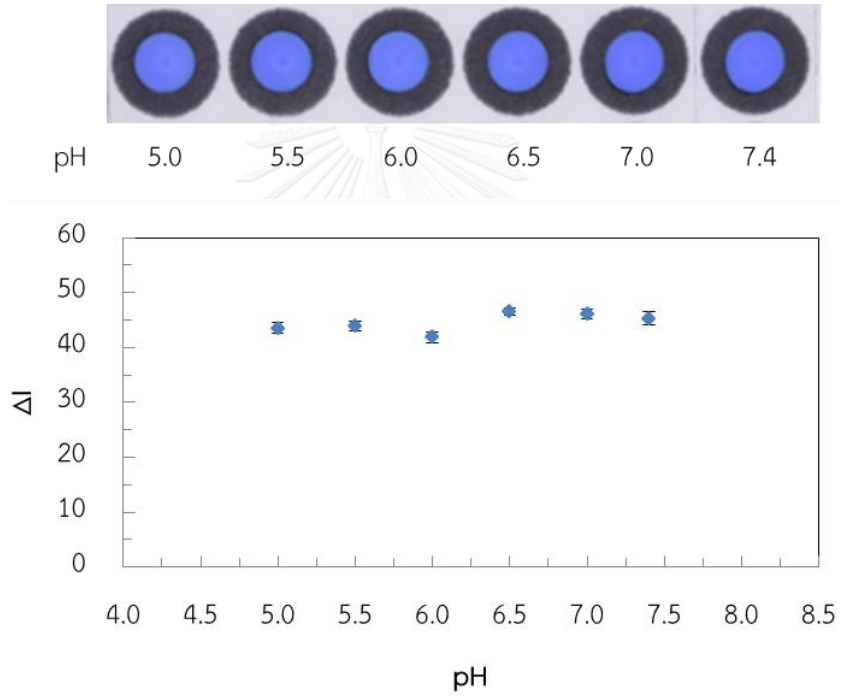

Figure 4.13 The observed color intensities of 40 ppm oxalate standard solution at different pH values.

4.7 Interference Study

For determination of oxalate in human urine using colorimetric detection based on the enzymatic reaction, the main components in urine including urea, AA, UA, CA, Cr and ALB were used to study the interfering effect on oxalate detection in urine. Concentrations of each component were prepared to cover the normal level found in normal human urine, as shown in Table 4.1, and mixed with 40 ppm oxalate.

Table 4.1 Concentration ranges of the main components found in urine for interference study.

Components	Normal levels (ppm)	Prepared concentration range (ppm)
Urea	20,000	4,000 - 24,000
AA	600	40 - 800
UA	600	40 - 800
CA	320	80 - 400
Cr	250	80 - 400
ALB	30	40 - 200

The obtained ΔI values of 40 ppm oxalate standard solution and the mixed solutions between 40 ppm oxalate and each component are shown in Figure 4.14. If the colorimetric determination of oxalate was not interfered by the main components in urine, the calculated %difference of the obtained ΔI values between 40 ppm oxalate standard solution and the mixed solutions should not be higher than 5% or should be in the ΔI range of 42.10 - 46.53. As seen from Figure 4.14, the color intensity of the mixed solution containing AA was not different from that of the background. This could be because AA as a reducing reagent was oxidized by H_2O_2,

which was generated from the enzymatic reaction between oxalate and OxOx, in the presence of HRP to produce a dehydroascorbic acid [74, 75], as shown in Figure 4.15. Accordingly, the color intensity was not observed because the produced H_2O_2 was completely reacted with AA in the solution instead of MBTH and DMAB in the reagent B.

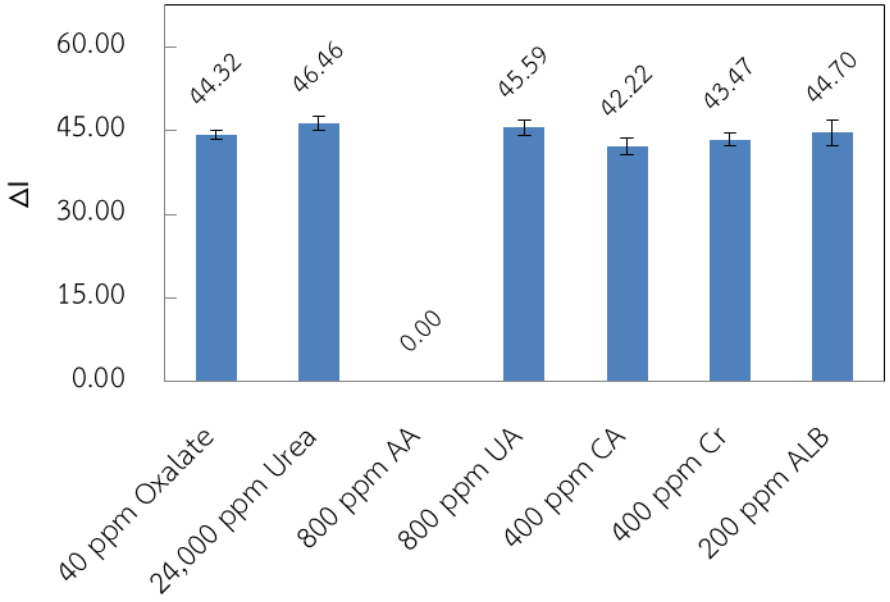

Figure 4.14 Effect of main components in urine on the colorimetric detection of oxalate based on the enzymatic reaction. Each component was mixed with 40 ppm oxalate.

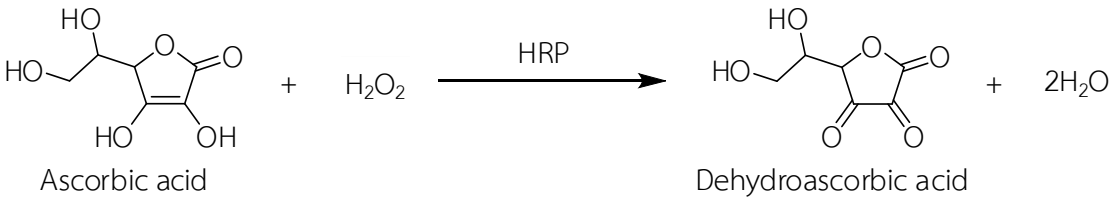

Figure 4.15 The oxidation of ascorbic acid using H_2O_2 as an oxidizing reagent in the presence of peroxidase to produce dehydroascorbic acid [76].

Since AA was an interfering component for the colorimetric detection of oxalate in urine based on the enzymatic reaction, a method to minimize the interfering effect of AA was studied.

4.7.1 Minimization of the Interfering Effect of AA Using Urine Dilution

To study the interfering effect of AA, 40 ppm oxalate as a normal oxalate level in human urine was mixed with different concentrations of AA. The %difference of ΔI values between 40 ppm oxalate and the mixed solutions was used to indicate the interfering level of AA. The %difference of ΔI higher than 5% indicated that AA interfered the colorimetric detection of oxalate. As shown in Figure 4.16 (a), the observed color intensity of each reaction between 40 ppm oxalate and different concentrations of AA was decreased when increasing AA concentration. The color intensities of each reservoir were measured to calculate ΔI values. A bar graph plotted between ΔI and AA concentration is shown in Figure 4.16 (b). The calculated %difference of ΔI of the mixed solution compared with 40 ppm oxalate was shown over each bar. The calculated %difference of ΔI lower than 5% was obtained when the AA level in samples was lower than 10 ppm. Therefore, the interfering effect of AA on oxalate detection was minimized using 120-fold urine dilution to dilute the normal level of AA from 600 ppm to 5 ppm.

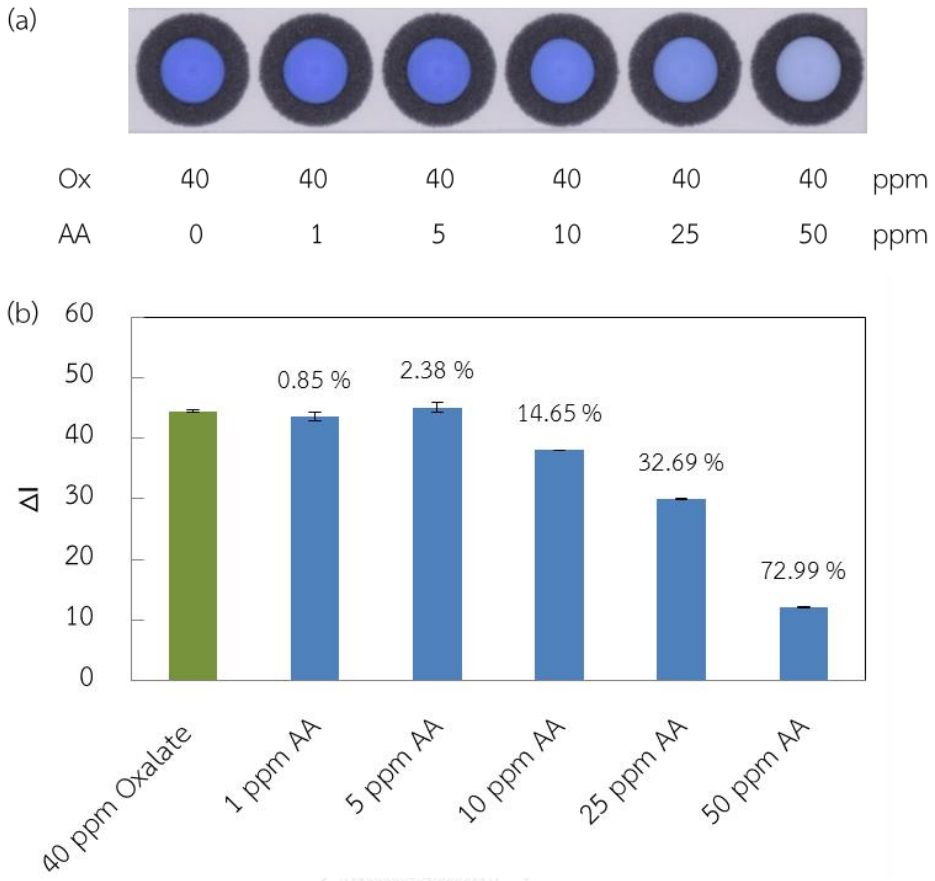

Figure 4.16 Effect of concentration on the observed color intensities of oxalate detection (a). The obtained ΔI values were plotted as a function of AA concentration in the mixed solutions and the calculated %difference was shown over each bar graph (b).

Although the interfering effect of AA could be minimized using 120 folds dilution of urine (AA was diluted from 600 to 5 ppm), the oxalate content was also diluted to 0.33 ppm (oxalate was diluted from 40 ppm, which is the normal level of oxalate in urine of healthy people) which was lower than the LOD value (3.38 ppm). Therefore, urine could not be diluted 120 folds to minimize the interfering effect of AA on oxalate detection.

4.7.2 Minimization of the Interfering Effect of AA Using a Masking Reagent

Alternatively, AA could be eliminated using an oxidizing reagent because AA is a reducing reagent. Zhu et al. [75] reported the minimization of interfering effect of AA on the determination of thiamine in pharmaceutical samples using difference masking reagents as oxidizing reagents. The fluorescence intensity of 1 ppm thiamine between with and without 40 ppm AA was not significantly different when using Cu^{2+} (25 ppm) and H_3BO_3 (0.12 M)-NaOH (0.014 M) as a masking reagent. The interfering effect of AA was minimized because AA was oxidized by Cu^{2+} to produce dehydroascorbic acid and the product was reacted with H_3BO_3 to form a complex, as shown in Figure 4.17.

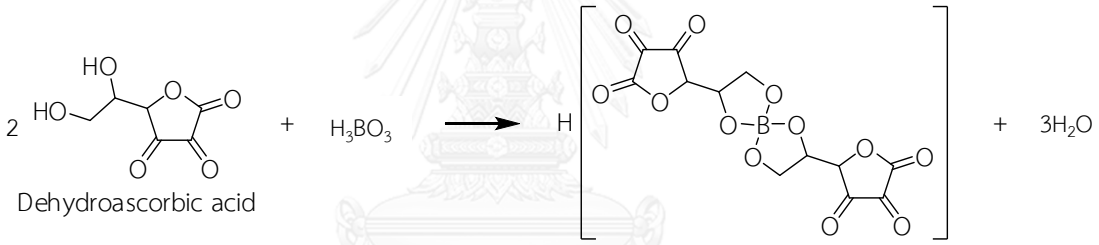

Figure 4.17 The complex formation between dehydroascorbic acid and H_3BO_3 [77].

Therefore, 25 ppm Cu^{2+} and H_3BO_3 (0.12 M)-NaOH (0.014 M) were applied in this work as a masking reagent to minimize the interfering effect of AA on the oxalate detection.

From the previous work, the masking time (reaction time of AA, Cu^{2+} and H_3BO_3-NaOH) of 30 min at room temperature was used to minimize the interfering effect of 40 ppm AA. However, the normal level of AA in urine is higher than the interfering level (40 ppm) of AA in the previous work. Therefore, optimization of masking time to minimize the interfering effect of AA was studied.

For optimization of the masking time, the masking reagent was added into mixed solutions of 40 ppm oxalate and AA at different concentrations in safe-lock tubes. The mixed solutions were incubated at room temperature using the masking times of 10, 20, 30, 40, 50 and 60 min and then pipetted to mix with reagents A and B. Photographs of each reaction at different masking times taken at 10 min reaction time are shown in Figure 4.18 (a). The color intensity of the mixed solutions between 40 ppm oxalate and AA at different concentrations was increased when increasing the masking time. Although the interfering effect of AA was minimized when increasing the masking time, less analysis time was preferable for onsite detection. Accordingly, sample dilution was used together with the masking reagent to minimize the interfering effect of AA to reduce the masking time. Since the normal level of oxalate in urine was 40 ppm and LOD of oxalate detection using this method is 3.55 ppm, the concentration of oxalate after urine dilution should not be lower than LOD. Therefore, the dilution of urine was selected to be 5 folds. Accordingly, the levels of oxalate and AA were diluted to 8 and 120 ppm, respectively, from the normal levels found in urine of healthy people. It was found that at 120 ppm AA, the calculated %difference was lower than 5% when using the masking time longer than 20 min, as shown in Figure 4.18 (b). Therefore, the masking time of 30 min was used to ensure that AA did not interfere the colorimetric detection of oxalate.

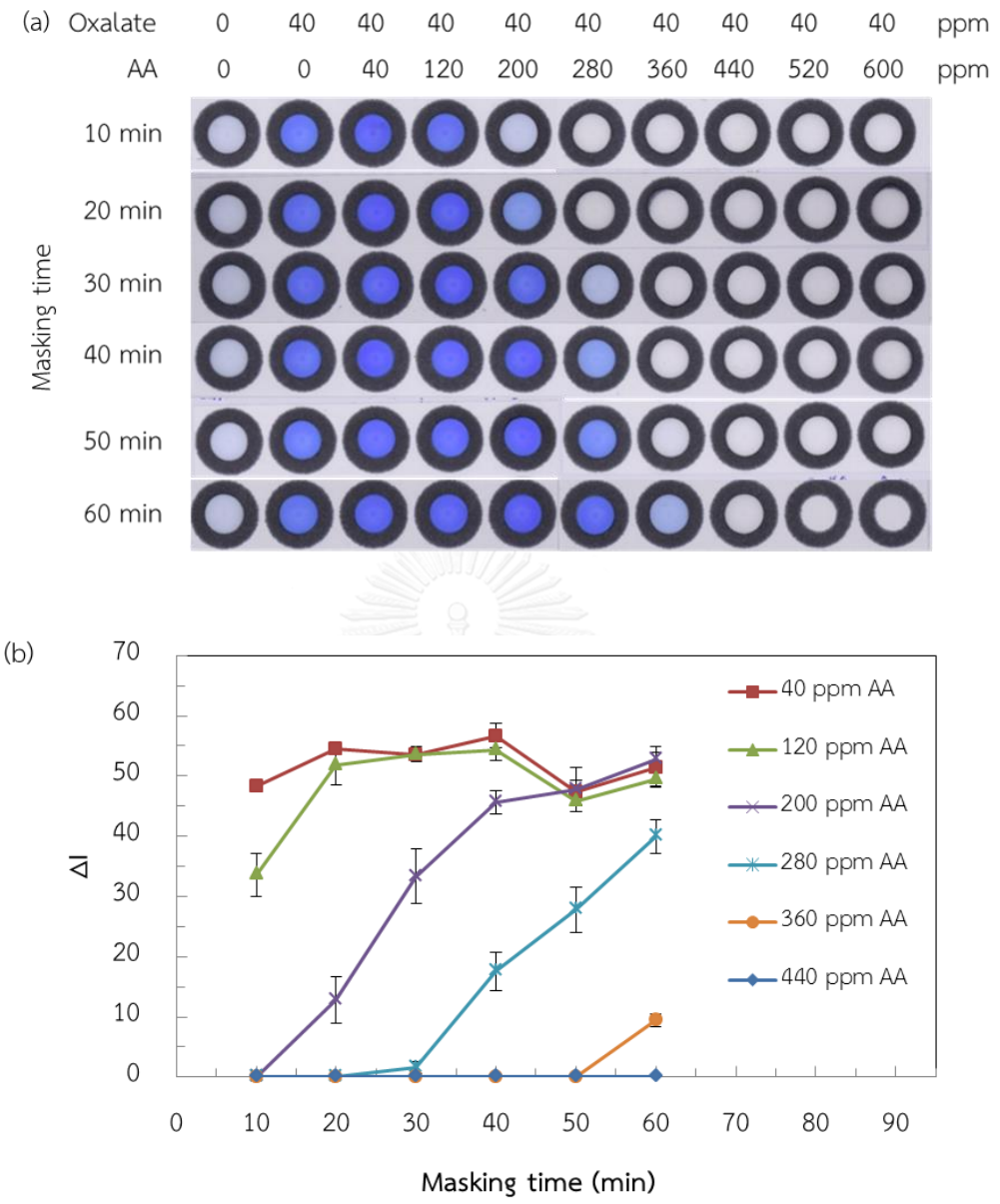

Figure 4.18 (a) The color intensities of the mixed solutions between 40 ppm oxalate and AA at different concentrations and different masking times. (b) The obtained ΔI values of the mixed solutions were plotted as a function of masking time.

It was concluded that the interfering effect of AA on oxalate detection in urine was minimized using the masking reagent of 25 ppm Cu^{2+} and H_3BO_3 (0.12 M)-NaOH (0.014 M) at a 30 min masking time together with 5-fold urine dilution.

4.8 Analytical Performance

4.8.1 Linearity and Calibration Curve

A linear range of oxalate concentration was studied using the oxalate concentration range of 5 to 1,000 ppm to perform the reaction under the optimized conditions. As shown in Figure 4.19 (a), the observed color intensities were increased when increasing oxalate concentration to react with reagents A and B. The linearity was observed in the concentration range of 5 to 50 ppm, as shown in the inset of Figure 4.19 (b), with a linear equation of y = 1.2045x + 0.9141 and a correlation coefficient (R^2) of 0.9968.

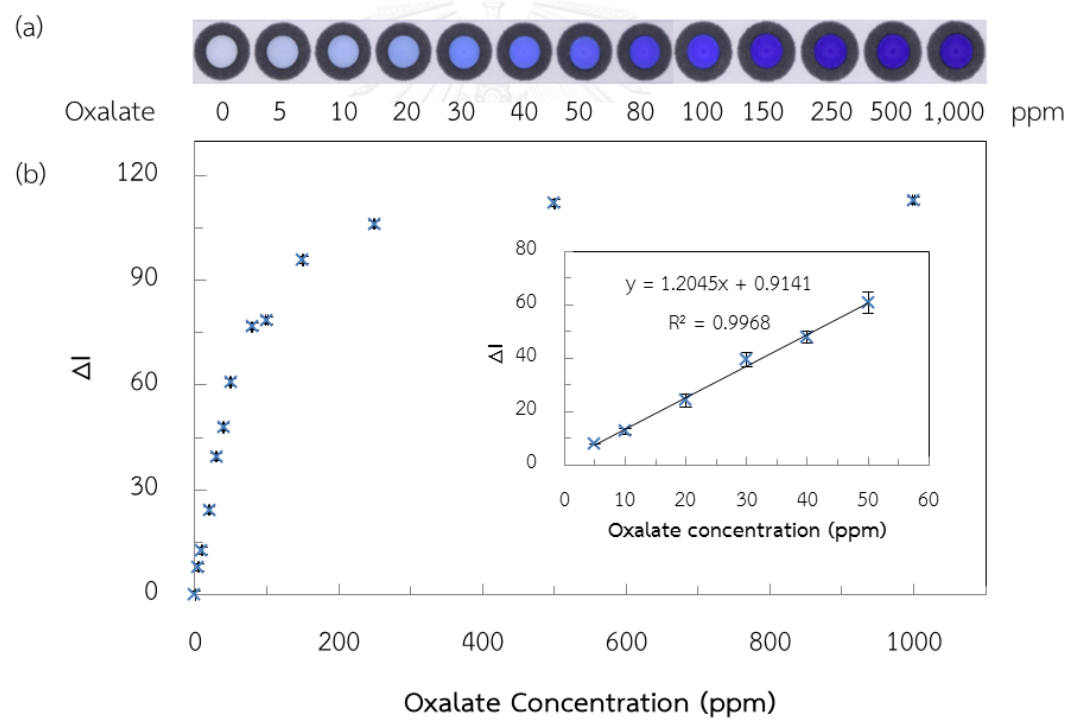

Figure 4.19 (a) The observed color intensities of oxalate at difference concentrations. The ΔI values were plotted versus oxalate concentration. The linear relationship (shown in the inset) was in the concentration range of 5 to 50 ppm.

4.8.2 Limit of Detection (LOD) and Limit of Quantitation (LOQ)

The LOD and LOQ were calculated from 3 and 10 times of standard deviation (SD) divided by the slope of the linear equation, respectively. The calculated LOD and LOQ found to be 3.38 and 11.27 ppm, respectively.

4.8.3 Accuracy

To verify the accuracy of this method for determination of oxalate in urine, oxalate standard solution at 3 concentration levels of 5, 15 and 30 ppm was added into 10 urine samples containing the masking reagent. Each solution was reacted with reagents A and B using the optimized conditions. The obtained ΔI of each solution was used to calculate %recovery using Equation 3.5. As shown in Table 4.2, the calculated %recovery was in the range of 80.73-110.00 %, which was acceptable according to the Association of Official Agriculture Chemists (AOAC) [78] which set the acceptable range of 80-110 %. Therefore, this method showed acceptable accuracy for determination of oxalate in urine.

Table 4.2 Percent recovery of oxalate standard solutions spiked into urine samples.

Sample No.	Oxalate (ppm)		%Recovery	Sample No.	Oxalate (ppm)		%Recovery
	Added	Found ± SD			Added	Found ± SD	
1	0	5.60 ± 0.10	-	6	0	4.88 ± 0.85	-
	5	10.74 ± 0.62	102.76		5	9.22 ± 1.12	86.68
	15	21.94 ± 0.10	108.92		15	21.17 ± 1.74	108.55
	30	36.87 ± 1.44	104.25		30	36.39 ± 0.15	105.02
2	0	19.90 ± 0.93	-	7	0	0.86 ± 0.36	-
	5	24.88 ± 0.38	99.60		5	5.10 ± 1.65	84.91
	15	34.65 ± 1.11	98.33		15	17.08 ± 1.75	108.18
	30	47.94 ± 4.76	93.48		30	31.80 ± 1.09	103.16
3	0	2.98 ± 0.39	-	8	0	3.74 ± 0.11	-
	5	7.11 ± 2.07	82.73		5	8.17 ± 0.45	88.47
	15	18.97 ± 0.15	106.63		15	19.18 ± 0.52	102.88
	30	34.47 ± 2.40	105.00		30	36.70 ± 0.64	109.84
4	0	2.45 ± 0.22	-	9	0	0.71 ± 0.12	-
	5	6.71 ± 0.54	85.22		5	5.72 ± 1.10	100.28
	15	18.60 ± 0.78	107.66		15	17.10 ± 1.36	109.24
	30	35.45 ± 0.64	110.00		30	32.97 ± 1.76	107.55
5	0	9.47 ± 0.92	-	10	0	3.83 ± 0.33	-
	5	14.74 ± 0.88	105.38		5	8.99 ± 1.18	103.15
	15	25.49 ± 0.68	106.80		15	19.67 ± 2.07	105.58
	30	38.37 ± 2.76	96.34		30	36.11 ± 2.75	107.58

4.8.4 Precision

The precision of the method was investigated for both inter-day and intra-day precisions. For Intra-day precision, the determination of oxalate in a urine sample was repeated for 11 times. Furthermore, the determination of oxalate in the same urine sample was repeated for 3 days to observe inter-day precision.

4.8.4.1 Intra-day Precision

For intra-day precision, oxalate concentrations of 5, 15 and 30 ppm were added into urine samples containing the masking reagent. The amounts of oxalate in samples and the spiked samples were determined for 11 times using the optimized conditions. The obtained ΔI values were plotted versus the number of experiment, as shown in Figure 4.20.

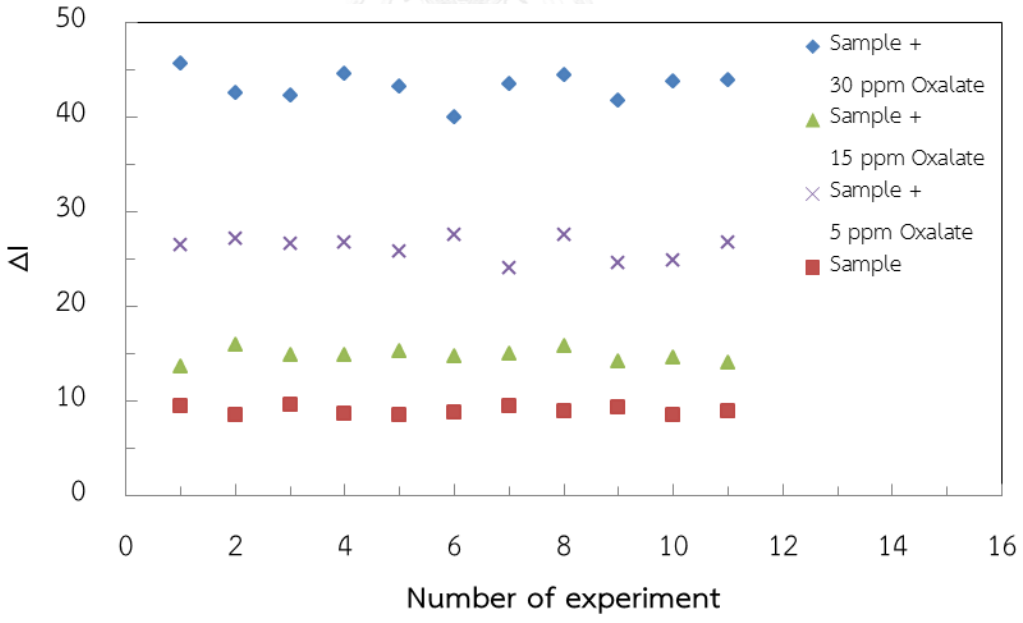

Figure 4.20 Intra-day determination of oxalate in urine and urine added with 5, 15 and 30 ppm oxalate using the optimized conditions. Each sample was measured for 11 times.

The obtained ΔI values of sample and each spiked sample were used to calculate %RSD using Equation 3.6. The calculated %RSD values were found to be lower than 5%, which was acceptable according to AOAC [78], which limits %RSD to be lower than 8%.

4.8.4.2 Inter-day Precision

The solution preparation for inter-day detection of oxalate was similar to that of the intra-day detection of oxalate, but the determination of oxalate in urine for inter-day precision was examined for 3 days and 3 replicates for each day. The obtained ΔI values from each day were shown in Figure 4.21.

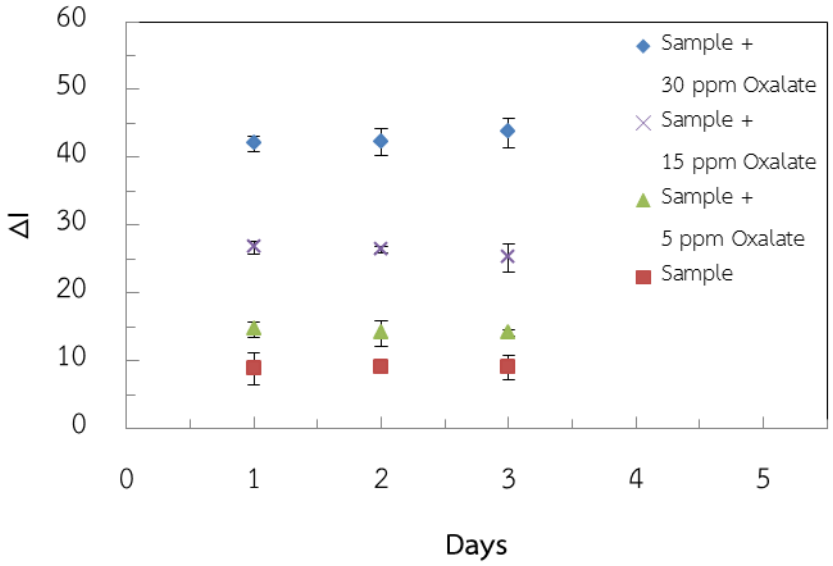

Figure 4.21 The inter-day determination of oxalate in urine and urine added with 5, 15 and 30 ppm oxalate using the optimized conditions. The experiments were repeated for 3 days and 3 replicates for each day.

Similar to intra-day precision, the obtained ΔI values were used to calculate %RSD. The calculated %RSD values for inter-day detection of oxalate in urine were found to be lower than 4%, which was acceptable according to the AOAC [78].

4.9 Determination of Oxalate in Urine Samples

Determination of oxalate in urine samples using PADs was performed using the optimized conditions. To validate that this method is reliable, UV-Vis spectrophotometry was used to measure the amount of oxalate in urine samples using an oxalate kit as a standard method. A calibration curve of UV-Vis spectrophotometric method was constructed using absorbance plotted versus oxalate concentration in the range of 10 to 100 ppm, as shown in Figure 4.22.

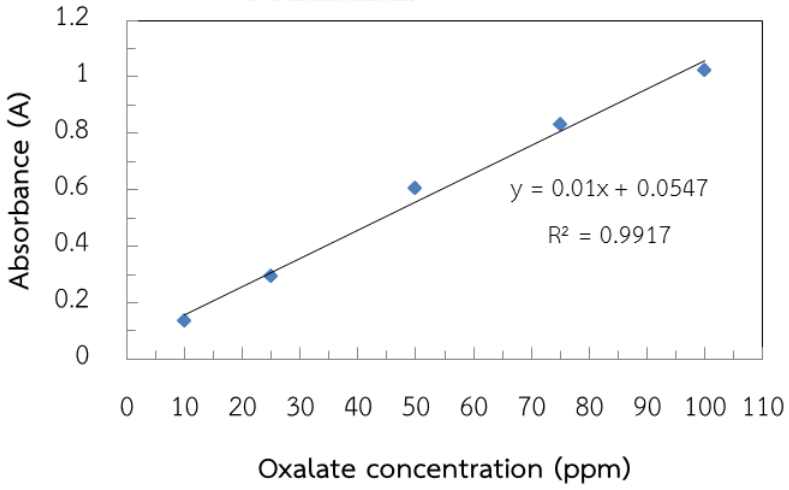

Figure 4.22 A calibration plot of absorbance as a function of oxalate concentration for quantitative determination of oxalate.

The same urine samples used in oxalate detection using PADs were measured for absorbance values. The absorbance was converted to oxalate concentration using the linear equation of the calibration curve shown in Figure 4.22. After that, the obtained oxalate concentrations in each urine sample from both methods were compared using the paired student t-test, as shown in Table 4.3.

Table 4.3 The comparison of oxalate concentrations in urine samples obtained from PADs and UV-Vis spectrophotometry as a standard method (n=10).

Sample	Oxalate (ppm)	
	PADs ± SD	UV-Vis spectrophotometry ± SD
1	27.99 ± 0.51	29.38 ± 0.01
2	99.50 ± 4.67	104.74 ± 0.02
3	14.88 ± 1.95	12.56 ± 0.02
4	12.24 ± 1.12	13.47 ± 0.11
5	47.35 ± 4.61	42.05 ± 0.02
6	24.43 ± 4.24	20.18 ± 0.01
7	4.28 ± 1.78	5.56 ± 0.03
8	18.73 ± 0.54	17.14 ± 0.22
9	3.55 ± 0.62	4.01 ± 0.01
10	19.17 ± 1.66	22.27 ± 0.01

For the paired student t-test, the calculated mean of oxalate obtained from PADs was compared with the standard method. The reliability of the PADs for determination of oxalate in urine sample was verified using a comparison of t-value and t-critical. If t-value was lower than t-critical, the obtained oxalate concentrations from the PADs were not significantly different from that of the standard method and acceptable for determination of oxalate in urine samples.

In this work, the t-critical was 2.26 at a 95% confident interval (n = 10) and the t-value was found to be 1.09, which lower than the t-critical. Therefore, the proposed approach using PADs was a reliable method for determination of oxalate in urine samples.

In addition, the linear regression analysis was used to confirm the reliability of the PADs for determination of oxalate in urine samples. The obtained amounts of oxalate found in each urine sample using this method were plotted with the amounts of oxalate found in the same samples obtained from the standard method, as shown in Figure 4.23. If a correlation coefficient (R^2) was closer to 1 and a significance F was lower than 0.05, this method is reliable for determination of oxalate in urine samples. From the linear regression analysis at a 95% confident interval, a correlation coefficient (R^2) was found to be 0.9874 and a calculated significance F was lower than 0.05. Accordingly, this method was reliable when compared with a standard method for determination of oxalate in urine samples [79, 80].

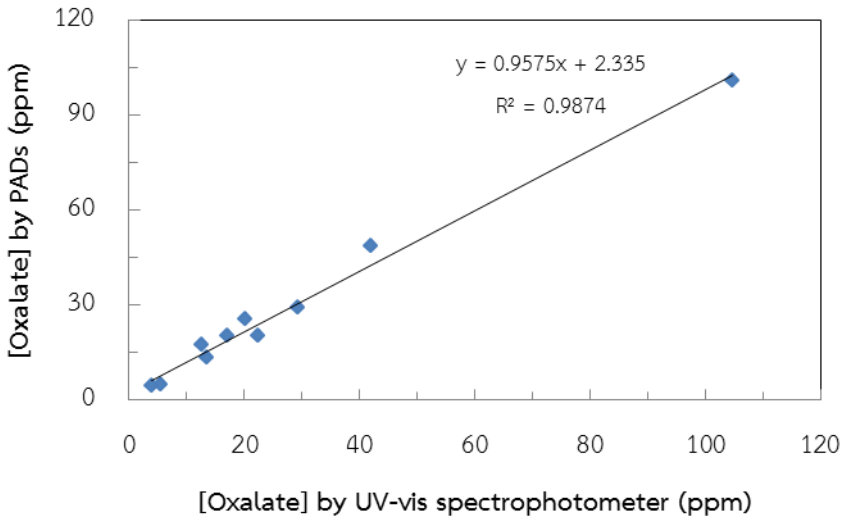

Figure 4.23 The relationship of the amounts of oxalate in urine samples obtained from PADs and those from the UV-Vis spectrophotometry as a standard method.

CHAPTER V
CONCLUSIONS AND FUTURE WORK

In this work, oxalate sensors based on the enzymatic reaction between oxalate and OxOx were developed using electrochemical and colorimetric detections separately coupled with PADs.

For electrochemical detection, CV was used to optimize carbon paste composition for fabrication of CPEs on paper. The optimized compositions were 50% w/w oil phase and 50% w/w graphite powder, in which the oil phase was composed of 50% w/w mineral oil and 50% w/w PDMS. The amounts of AgNPs and MWCNTs were also optimized for the modification of CPEs. A AgNPs-MWCNTs-CPE was obtained from the CPE modified with 400 µL of 10,000 ppm AgNPs and 1% w/w MWCNTs. The AgNPs-MWCNTs-CPE was used as a WE for determination of oxalate in urine through the amperometric measurements of H_2O_2 generated from the enzymatic reaction. For amperometric measurements, a plot of S/B ratios and applied potentials as a hydrodynamic voltammogram was used to determine an optimum applied potential, which found to be -0.6 V. Under the optimized conditions, two linearity ranges were obtained in the ranges of 0.05-10 and 10-1,000 mM. The calculated LOD and LOQ were found to be 0.02 and 0.08 ppm, respectively. These experiments confirmed that H_2O_2 could be measured using the AgNPs-MWCNTs-CPE with amperometric detection. However, when measuring oxalate using the enzymatic reaction, no current was observed. This could be because the H_2O_2 produced from the enzymatic reaction was simultaneously reacted with HRP contained in a regent B to produce H_2O and the oxidized form of HRP. Therefore, the determination of oxalate using PADs with electrochemical detection was not successful.

Another method for determination of oxalate based on the enzymatic reaction was also developed using PADs coupled with colorimetric detection. The

optimized amount of reagent A, reagent B and sample were 30, 5 and 5 µL, respectively. The highest color intensity was obtained when using 10 min of reaction time at room temperature. From the interference study, only AA in urine could interfere the determination of oxalate using the proposed approach. Therefore, a masking reagent consisting of 25 ppm Cu^{2+} and H_3BO_3 (0.12 M)-NaOH (0.014 M) was added in 5-fold diluted urine samples to minimize interfering effect of AA. Under the optimized conditions, a linearity range of this method was in the range of 5-50 ppm. LOD and LOQ were found to be 3.38 and 11.27 ppm, respectively. Accuracy of the method was evaluated using %recovery of oxalate standard solutions spiked in urine. It was found that %recovery was in the range of 80.73-110.00 %. Intra-day and inter-day precisions were investigated from %RSD of the amount of oxalate found in samples, which were found to be lower than 5% and 4%, respectively. In addition, oxalate concentrations obtained from this method were compared with those from UV-Vis spectrophotometry, which was used as a standard method, using the student t-test and intra-class correlation coefficient at a 95% confident interval. The obtained t-value (1.09) was lower than t-critical (2.26) and the correlation coefficient (R^2) was found to be 0.9874, which was in the acceptable range (0.81-0.98). Therefore, the proposed approach using PADs was a reliable method for determination of oxalate in urine samples.

Although the PADs coupled with electrochemical detection was not successfully to determine oxalate in the solution due to the limitation of the mixed reagent B, the colorimetric detection of oxalate was successful to determine the amount of oxalate in urine with high accuracy and precision.

The determination of oxalate based on the enzymatic reaction using ePADs is an interesting method because electrochemical detection provides high selectivity and sensitivity. However, the H_2O_2 generated from the enzymatic reaction was reacted with HRP to produce the oxidized form of HRP. An alternative method for electrochemical determination of oxalate is to use a mediator to react with the oxidized form of HRP to produce the oxidized form of mediator. After that, the reduction of the oxidized mediator occurs at the electrode surface. Therefore, the

electrochemical signal could be observed from the electron transfer at the electrode surface. Accordingly, future works could be the development of ePADs for determination oxalate based on the enzymatic reaction using a mediator. However, the AgNPs-MWCNTs-CPE might not be suitable for the new system. Therefore, new modifiers will be also considered for CPE modification.

REFERENCES

[1] Byham-Gray, L.D., Burrowes, J.D., and Chertow, G.M. Nutrition in kidney disease. 2, Editor. 2014, Springer Science + Business Media: USA.

[2] Chanapa, P. The risk factors of kidney stones focusing on calcium and oxalate. Songklanagarind Medical Journal 29(6) (2011): 299-308.

[3] Sidorova, A.A. and Grigoriev, A.V. Determination of diagnostical markers of urolithiasis by capillary electrophoresis. Journal of Analytical Chemistry 67(5) (2012): 478-485.

[4] Perello, J., Sanchis, P., and Grases, F. Determination of uric acid in urine, saliva and calcium oxalate renal calculi by high-performance liquid chromatography/mass spectrometry. Journal of chromatography. B, Analytical technologies in the biomedical and life sciences 824(1-2) (2005): 175-80.

[5] Maya, F., Estela, J.M., and Cerdà, V. Multisyringe ion chromatography with chemiluminescence detection for the determination of oxalate in beer and urine samples. Microchimica Acta 173(1-2) (2010): 33-41.

[6] Elgstoen, K.B., Woldseth, B., Hoie, K., and Morkrid, L. Liquid chromatography-tandem mass spectrometry determination of oxalate in spot urine. Scandinavian Journal of Clinical and Laboratory Investigation 70(3) (2010): 145-50.

[7] Tabe, M., Fujimoto, T., Nakahara, R., Yamaguchi, T., and Fujita, Y. Spectrophotometric determination of oxalate ion with N,N′-Diethyl-N,N′- [4,4′-dihydroxy-1,1′-binaphthalene]-3,3′-diyl]bisbenzamide and Copper(II). Analytical Sciences 23 (2007): 601-604.

[8] March, J.G., Simonet, B.M., Grases, F., Munoz, J.A., and Valiente, M. Determination of trace amounts of oxalate in renal calculi and related samples by gas chromatography-mass spectrometry. Chromatographia 57 (2003): 811-817.

[9] Munoz, J.A., Canpana, A.M.G., and Barrero, F.A. Effect of cationic micelles on the formation of the complex oxalate–Alizarin Red S–Zr(IV) Application to the

sensitive fluorescence determination of oxalate ion. Talanta 47 (1998): 387-399.

[10] Mishra, R., Yadav, H., and Pundir, C.S. An amperometric oxalate biosensor based on sorghum leaf oxalate oxidase immobilized on carbon paste electrode. analytical letters 43(1) (2010): 151-160.

[11] Rodriguez, J.A., Hernandez, P., Salazar, V., Castrillejo, Y., and Barrado, E. Amperometric biosensor for oxalate determination in urine using sequential injection analysis. Molecules 17(12) (2012): 8859-8871.

[12] Brasselet, C., et al. Prepercutaneous coronary intervention plasma homocysteine concentration is a useful predictor of angioplasty-induced myocardial damage. Clinical Chemistry 51(12) (2005): 2374-7.

[13] Pundir, C.S. and Sharma, M. Oxalate biosensor: a review. Journal of Scientific & Industrial Research 69 (2010): 489-494.

[14] Fiorito, P.A. and Cordoba de Torresi, S.I. Optimized multilayer oxalate biosensor. Talanta 62(3) (2004): 649-54.

[15] Milardovic, S., Kerekovic, I., and Nodilo, M. A novel biamperometric biosensor for urinary oxalate determination using flow-injection analysis. Talanta 77(1) (2008): 222-8.

[16] Devi, R., Relhan, S., and Pundir, C.S. Construction of a chitosan/polyaniline/graphene oxide nanoparticles/polypyrrole/Au electrode for amperometric determination of urinary/plasma oxalate. Sensors and Actuators B: Chemical 186 (2013): 17-26.

[17] Yadav, S., Devi, R., Kumari, S., Yadav, S., and Pundir, C.S. An amperometric oxalate biosensor based on sorghum oxalate oxidase bound carboxylated multiwalled carbon nanotubes-polyaniline composite film. Journal of Biotechnology 151(2) (2011): 212-7.

[18] Pundir, C.S., Chauhan, N., Rajneesh, Verma, M., and Ravi. A novel amperometric biosensor for oxalate determination using multi-walled carbon nanotube-gold nanoparticle composite. Sensors and Actuators B: Chemical 155(2) (2011): 796-803.

[19] Chauhan, N., Narang, J., Shweta, and Pundir, C.S. Immobilization of barley oxalate oxidase onto gold-nanoparticle-porous CaCO(3) microsphere hybrid for amperometric determination of oxalate in biological materials. Clinical Biochemistry 45(3) (2012): 253-8.

[20] Afraz, A., Rafati, A., and Hajian, A. Analytical sensing of hydrogen peroxide on Ag nanoparticles–multiwalled carbon nanotube-modified glassy carbon electrode. Journal of Solid State Electrochemistry 17(7) (2013): 2017-2025.

[21] Yang, P., Wei, W., Tao, C., Xie, B., and Chen, X. Nano-silver/multi-walled carbon nanotube composite films for hydrogen peroxide electroanalysis. Microchimica Acta 162(1-2) (2007): 51-56.

[22] Bedin, F., Boulet, L., Voilin, E., Theillet, G., Rubens, A., and Rozand, C. Paper-based point-of-care testing for cost-effective diagnosis of acute flavivirus infections. Journal of Medical Virology 9999 (2017): 1-8.

[23] Cinti, S., Basso, M., Moscone, D., and Arduini, F. A paper-based nanomodified electrochemical biosensor for ethanol detection in beers. Analytica Chimica Acta 960 (2017): 123-130.

[24] Weaver, A.A., Halweg, S., Joyce, M., Lieberman, M., and Goodson, H.V. Incorporating yeast biosensors into paper-based analytical tools for pharmaceutical analysis. Analytical and Bioanalytical Chemistry 407(2) (2015): 615-9.

[25] Liang, L., et al. Aptamer-based fluorescent and visual biosensor for multiplexed monitoring of cancer cells in microfluidic paper-based analytical devices. Sensors and Actuators B: Chemical 229 (2016): 347-354.

[26] Bui, M.P., Brockgreitens, J., Ahmed, S., and Abbas, A. Dual detection of nitrate and mercury in water using disposable electrochemical sensors. Biosensors and Bioelectronics 85 (2016): 280-6.

[27] Xu, Y., Liu, M., Kong, N., and Liu, J. Lab-on-paper micro- and nano-analytical devices: Fabrication, modification, detection and emerging applications. Microchimica Acta 183(5) (2016): 1521-1542.

[28] Abe, K., Suzuki, K., and Citterio, D. Inkjet-printed microfluidic multianalyte chemical sensing paper. Analytical Chemiatry 80 (2008): 6928–6934.

[29] Sun, L.-J., Xie, Y., Yan, Y.-F., Yang, H., Gu, H.-Y., and Bao, N. Paper-based analytical devices for direct electrochemical detection of free IAA and SA in plant samples with the weight of several milligrams. Sensors and Actuators B: Chemical 247 (2017): 336-342.

[30] Alahmad, W., Uraisin, K., Nacapricha, D., and Kaneta, T. A miniaturized chemiluminescence detection system for a microfluidic paper-based analytical device and its application to the determination of chromium(iii). Analytical Methods 8(27) (2016): 5414-5420.

[31] Petruci, J.F. and Cardoso, A.A. Portable and disposable paper-based fluorescent sensor for in situ gaseous hydrogen sulfide determination in near real-time. Anaytical Chemistry 88(23) (2016): 11714-11719.

[32] Zhang, X. and Ding, S.N. Graphite paper-based bipolar electrode electrochemiluminescence sensing platform. Biosensors and Bioelectronics 94 (2017): 47-55.

[33] Canales, B.K., Richards, N.G., and Peck, A.B. Rapid oxalate determination in blood and synthetic urine using a newly developed oxometer. Journal of Endourology 27(2) (2013): 145-8.

[34] Adkins, J., Boehle, K., and Henry, C. Electrochemical paper-based microfluidic devices. Electrophoresis 36(16) (2015): 1811-24.

[35] Santhiago, M., Wydallis, J.B., Kubota, L.T., and Henry, C.S. Construction and electrochemical characterization of microelectrodes for improved sensitivity in paper-based analytical devices. Analytical Chemistry 85(10) (2013): 5233-9.

[36] Martinez, A.W., Phillips, S.T., Butte, M.J., and Whitesides, G.M. Patterned paper as a platform for inexpensive, low-volume, portable bioassays. Angewandte Chemi International Edition 46(8) (2007): 1318-20.

[37] Nery, E.W. and Kubota, L.T. Sensing approaches on paper-based devices: a review. Analytical and Bioanalytical Chemistry 405(24) (2013): 7573-95.

[38] Xia, Y., Si, J., and Li, Z. Fabrication techniques for microfluidic paper-based analytical devices and their applications for biological testing: A review. Biosensors and Bioelectronics 77 (2016): 774-89.

[39] Li, X., Ballerini, D.R., and Shen, W. A perspective on paper-based microfluidics: current status and future trends. Biomicrofluidics 6(1) (2012): 11301-1130113.

[40] Liu, H. and Crooks, R.M. Paper-based electrochemical sensing platform with integral battery and electrochromic read-out. Analytical Chemistry 84(5) (2012): 2528-32.

[41] Dornelas, K.L., Dossi, N., and Piccin, E. A simple method for patterning poly(dimethylsiloxane) barriers in paper using contact-printing with low-cost rubber stamps. Analytica Chimica Acta 858 (2015): 82-90.

[42] Zhang, Y., et al. Equipment-free quantitative measurement for microfluidic paper-based analytical devices fabricated using the principles of movable-type printing. Analytical Chemistry 86(4) (2014): 2005-12.

[43] Songjaroen, T., Dungchai, W., Chailapakul, O., Henry, C.S., and Laiwattanapaisal, W. Blood separation on microfluidic paper-based analytical devices. Lab on aChip 12(18) (2012): 3392-8.

[44] Klasner, S.A., Price, A.K., Hoeman, K.W., Wilson, R.S., Bell, K.J., and Culbertson, C.T. Paper-based microfluidic devices for analysis of clinically relevant analytes present in urine and saliva. Analytical and Bioanalytical Chemistry 397(5) (2010): 1821-9.

[45] Dungchai, W., Chailapakul, O., and Henry, C.S. A low-cost, simple, and rapid fabrication method for paper-based microfluidics using wax screen-printing. Analyst 136(1) (2011): 77-82.

[46] Carrilho, E., Martinez, A.W., and Whitesides, G.M. Understanding wax printing: A simple micropatterning process for paper-based microfluidics. Analytical Chemistry 81(16) (2009): 7091-7095.

[47] Abe, K., Kotera, K., Suzuki, K., and Citterio, D. Inkjet-printed paperfluidic immuno-chemical sensing device. Analytical and Bioanalytical Chemistry 398(2) (2010): 885-93.

[48] Delaney, J.L., Hogan, C.F., Tian, J., and Shen, W. Electrogenerated chemiluminescence detection in paper-based microfluidic sensors. Analytical Chemistry 83(4) (2011): 1300-6.

[49] Olkkonen, J., Lehtinen, K., and Erho, T. Flexographically printed fluidic structures in paper. Analytical Chemistry 82(24) (2010): 10246-10250.

[50] Yu, J., Ge, L., Huang, J., Wang, S., and Ge, S. Microfluidic paper-based chemiluminescence biosensor for simultaneous determination of glucose and uric acid. Lab on aChip 11(7) (2011): 1286-91.

[51] Bracher, P.J., Gupta, M., Mack, E.T., and Whitesides, G.M. Heterogeneous films of ionotropic hydrogels fabricated from delivery templates of patterned paper. ACS Applied Materials & Interfaces 1(8) (2009): 1807-12.

[52] Cate, D.M., Adkins, J.A., Mettakoonpitak, J., and Henry, C.S. Recent developments in paper-based microfluidic devices. Analytical Chemistry 87(1) (2015): 19-41.

[53] Lei, K.F. Chapter 1. Materials and Fabrication Techniques for Nano- and Microfluidic Devices. in *RSC Detection Science*, Labeed, F.H. and Fatoyinbo, H.O., Editors. 2014, The Royal Society of Chemistry 2015. 1-28.

[54] Liana, D.D., Raguse, B., Gooding, J.J., and Chow, E. Recent advances in paper-based sensors. Sensors (Basel) 12(9) (2012): 11505-26.

[55] Desmet, C., Marquette, C.A., Blum, L.J., and Doumeche, B. Paper electrodes for bioelectrochemistry: Biosensors and biofuel cells. Biosensors and Bioelectronics 76 (2016): 145-63.

[56] Bakker, E. and Qin, Y. Electrochemical sensors. Analytical Chemistry 78(12) (2006): 3965-3984.

[57] Skoog, D.A.W., D.M., Holler, F.J., and Crouch, S.R. Fundamentals of analytical chemistry. in 8 (ed.)Fundamentals of Analytical Chemistry, 2004.

[58] Kounaves, S.P. Voltammetric techniques. in Handbook of Instrumental Techniques for Analytical Chemistry.

[59] Wang, J. Analytical electrochemistry, ed. 2. New York: Wiley VCH, 2000.

[60] Das, S.D. Cyclic voltammetry [Online]. 2013

[61] Thomas, F.G. and Henze, G. Introdection to voltammetric analysis : Theory and practice. Australia: CSIRO, 2001.

[62] Adeloju, S.B. AMPEROMETRY. in Poole, P.W.T. (ed.)Encyclopedia of Analytical Science (Second Edition). Oxford: Elsevier, 2005.

[63] Garti, N., Tibika, F., Sarig, S., and Perlberg, S. The Inhibitory effect of poly polymetric carboxylic amio-acids. Biochemical and Biophysical Research Communications 97(3) (1980): 1154-1162.

[64] Laube, N., Jansen, B., and Hesse, A. Citric acid or citrates in urine which should we focus on in the prevention of calcium oxalate crystals and stones? Urological Research 30 (2002): 336 – 341.

[65] Klapkova, E., Fortova, M., Prusa, R., Moravcova, L., and Kotaska, K. Determination of urine albumin by new simple high-performance liquid chromatography method. Journal of Clinical Laboratory Analysis 30(6) (2016): 1226-1231.

[66] Laboratory tests [Online].

[67] Mazzachi, B.C., Teubner, J.K., and Ryall, R.L. The effect of ascorbic acid on urine oxalate measurement. Urolithiasis and Related Clinical Research (1985): 649-650.

[68] Sameenoi, Y., et al. Poly(dimethylsiloxane) cross-linked carbon paste electrodes for microfluidic electrochemical sensing. Analyst 136(15) (2011): 3177-84.

[69] Huang, Y., et al. Ultrasensitive cholesterol biosensor based on enzymatic silver deposition on gold nanoparticles modified screen-printed carbon electrode. Materials Science and Engineering: C 77 (2017): 1-8.

[70] Injang, U., Noyrod, P., Siangproh, W., Dungchai, W., Motomizu, S., and Chailapakul, O. Determination of trace heavy metals in herbs by sequential injection analysis-anodic stripping voltammetry using screen-printed carbon nanotubes electrodes. Analytical Chimica Acta 668(1) (2010): 54-60.

[71] Kamyabi, M.A. and Shafie, M.A. Electrocatalytic oxidation of dopamine, ascorbic acid and uric acid at electrocatalytic oxidation of dopamine, ascorbic acid and uric acid at poly-2,6-diaminopyridine on the surface of carbon nanotubes/GC electrodes. Journal of the Brazilian Chemical Society 23(4) (2012): 593-601.

[72] Nantaphol, S., Chailapakul, O., and Siangproh, W. Sensitive and selective electrochemical sensor using silver nanoparticles modified glassy carbon

electrode for determination of cholesterol in bovine serum. Sensors and Actuators B: Chemical 207 (2015): 193-198.

[73] Ahammad, A.J.S. Hydrogen peroxide biosensors based on horseradish peroxidase and hemoglobin. Journal of Biosensors & Bioelectronics s9 (2012): 1-11.

[74] Xu, J. and Jordan, R.B. Kinetics and mechanism of the reaction of aqueous copper(II) with ascorbic acid. Inorganic Chemistry 29(16) (1990): 2933-2936.

[75] Zhu, H., He, Q., Fang, Q., and Chen, H. Elimination of ascorbic acid interference with the determination of thiamine in pharmaceutical preparation by flow injection on-Line photochemical spectrofluorimetry. Analytical Letters 35(4) (2002): 707-720.

[76] Martinello, F. and Luiz da Silva, E. Mechanism of ascorbic acid interference in biochemical tests that use peroxide and peroxidase to generate chromophore. Clinica Chimica Acta 373(1-2) (2006): 108-16.

[77] Köse, D.A. and Zümreoglu-Karan, B. Complexation of boric acid with vitamin C. New Journal of Chemistry 33(9) (2009): 1874.

[78] Appendix F: Guidelines for standard method performance requirements. in AOAC Official Methods of Analysis, pp. 1-18, 2016.

[79] How to do regression analysis in microsoft excel [Online]. 2009. Available from: https://goople.wordpress.com/2009/04/09/%E0%B8%97%E0%B8%B3-regression-analysis-%E0%B9%83%E0%B8%99-microsoft-excel-%E0%B8%A7%E0%B8%B4%E0%B9%80%E0%B8%84%E0%B8%A3%E0%B8%B2%E0%B8%B0%E0%B8%AB%E0%B9%8C%E0%B8%AA%E0%B8%A1%E0%B8%81%E0%B8%B2/

[80] Regression [Online]. 2017. Available from: http://www.excel-easy.com/examples/regression.html

APPENDIX

VITA

Acting SubLit. Manassawee Janrod was born on Saturday 19th October 1991 in Bangkok, Thailand. In 2010, she graduated a high school level from a Science division of Chonradsadornumrung School, Chonburi, Thailand. She received a scholarship from the Science Achievement Scholarship of Thailand (SAST) to study Bachelor's degree in Chemistry at Burapha University, Chonburi, Thailand, and completed in 2014. After that, she studied a Master's Degree in Chemistry at the Faculty of Science, Chulalongkorn University, Bangkok, Thailand, with the same scholarship and completed in 2017.